

High energy scattering in QCD and cross singularities of Wilson loops

I. A. Korchemskaya *

*Dipartimento di Fisica, Università di Parma and
INFN, Gruppo Collegato di Parma, I-43100 Parma, Italy*

and

G. P. Korchemsky †

*Institute for Theoretical Physics,
State University of New York at Stony Brook,
Stony Brook, New York 11794 - 3840, U.S.A.*

Abstract

We consider elastic quark-quark scattering at high energy and fixed transferred momentum. Performing factorization of soft gluon exchanges into Wilson line expectation value we find that there is one-to-one correspondence between high energy asymptotics in QCD and renormalization properties of the so called cross singularities of Wilson lines. Using this relation we show that the asymptotic behavior of the quark-quark scattering amplitude is controlled by a 2×2 matrix of the cross anomalous dimensions. We evaluate the matrix of cross anomalous dimension to two-loop order and study the properties of the obtained expressions to higher loop order.

*On leave from the Moscow Energetic Institute, Moscow, Russia

†On leave from the Laboratory of Theoretical Physics, JINR, Dubna, Russia

1. Introduction

Recent experimental data from Tevatron and HERA renewed our interest to theoretical interpretation of the well known phenomena in the physics of strong interactions like growth of the total hadronic cross section at high energy and increasing of the structure function of deep inelastic scattering at small values of the Bjorken variable x . In both cases we deal with the asymptotic behavior of hadronic scattering amplitudes at high energy s and fixed transferred momenta t the so called Regge behavior in high-energy QCD [1]. This problem is one of the longstanding in QCD and previous attempts to solve it have led to the discovery of the BFKL pomeron [2]. However, found in the leading logarithmic approximation, $\alpha_s \ll 1$ and $\alpha_s \log s \sim 1$, the BFKL pomeron leads to the expressions for the scattering amplitudes which violate the unitarity Froissart bound. To preserve the unitarity of the S -matrix, one has to go beyond the leading logarithmic approximation calculating the scattering amplitudes. The problem turns out to be very complicated and the following approaches have been proposed:

- Generalized leading logarithmic approximation [3, 4], in which we start with the leading logarithmic result and add “minimal” number of nonleading corrections in order to unitarize the result;
- Two-dimensional reggeon field theory [5], in which the high-energy scattering of gluons is described by the S -matrix of the effective two-dimensional field theory corresponding to dynamics of transverse gluonic degrees of freedom;
- Quasielastic unitarity approximation [6], in which one takes into account only contributions of soft gluons with transverse momenta much smaller hadronic scale.

These schemes are approximate and they were developed to resum special class of corrections which are expected to determine the high-energy asymptotics of the scattering amplitudes. In each case, QCD is replaced by simplified effective theory which inherits a rich structure of the original theory.

Recently [7, 8], a progress has been made using the generalized leading logarithmic approximation. It was found that in this approximation high energy QCD turns out to be a completely integrable model equivalent to the one-dimensional Heisenberg magnet of spin $s = 0$. This opens the possibility to apply powerful quantum inverse scattering method and calculate the hadronic scattering amplitudes by means of the Generalized Bethe Ansatz [8].

There were different proposals for the effective two-dimensional reggeon field theory [5, 9] and the hope is that the model can be solved exactly. Although to the lowest order of PT the effective reggeon theory reproduces the QCD expressions for the scattering amplitudes, the all order perturbative solution is not available yet.

The present paper is devoted to the calculation of the hadronic scattering amplitudes in the quasielastic unitarity approximation [6]. In this approximation, we use the parton model and approximate the hadron-hadron interaction as the scattering of partons. Partons interact with each other by exchanging soft gluons with energy which is much smaller than parton energy, s , but much bigger than the QCD scale Λ_{QCD} in order for the perturbative QCD to be applicable. Being calculated to the lowest orders of PT, the parton-parton scattering amplitudes get large perturbative corrections $(\alpha_s \log s \log t)^n$ due to soft gluon exchanges [6] and these Sudakov logarithms need to be resummed to all orders of PT. The resummation of leading logarithmic corrections can be performed using the “evolution equation” technique [6, 10] but we don't

have a regular way to resum and control nonleading logarithmic corrections to the scattering amplitude. A new approach which enables us to take into account systematically both leading and nonleading logarithmic corrections to the parton-parton scattering amplitudes has been proposed in [11]. In this approach, the partonic scattering in QCD is described by the dynamics of the gauge invariant collective variables defined as

$$W = W(C_1, C_2, \dots, C_n) \equiv \langle 0|T \operatorname{tr}_{R_1} P e^{ig \oint_{C_1} dx \cdot A(x)} \dots \operatorname{tr}_{R_n} P e^{ig \oint_{C_n} dx \cdot A(x)} |0\rangle, \quad (1.1)$$

the so called *Wilson loop functions*. Here, the path-ordered exponentials are evaluated along the closed paths $C_1 \dots C_n$ in Minkowski space-time and the gauge fields are defined in the irreducible representations $R_1 \dots R_n$ of the $SU(N)$ gauge group. One should stress that it is not for the first time when one dealt with this object. There were attempts [12] in 80's to study the nonperturbative dynamics of QCD in terms of Wilson loops. The interest to the Wilson loops was renewed after it was recognized [13] that the same loop functions enter into consideration in perturbative QCD when we study the effects of soft gluons in hardonic processes. Interacting with soft gluons described by gauge field $A_\mu(x)$, partons behave as relativistic charged classical particles and the path-ordered exponentials appear as eikonal phases of partons. The integration paths $C_1 \dots C_n$ have a meaning of semi-classical trajectories of partons and the choice of the representations $R_1 \dots R_n$ is fixed by their charges. In particular, R is fundamental and adjoint representation of the $SU(N)$ group for quarks and gluons, respectively.

The paper is organized as follows. In sect.2 we consider the amplitude of near forward elastic quark-quark scattering and show its relation with the renormalization properties of the so called cross singularities of Wilson loops. In sects.3 and 4 we analyze the cross singularities of Wilson loops to the lowest orders of PT and find two-loop expression for the matrix of cross anomalous dimensions. The properties of the obtained expressions which can be generalized to all orders of PT are studied in sect.5. The details of the calculations of the two-loop Feynman diagrams contributing to the Wilson lines are given in Appendices A and B. Large N limit of the Wilson line is analysed in Appendix C.

2. High energy scattering in QCD

Let us briefly summarize the results of the paper [11] concerning the relation between high energy behavior of the scattering amplitudes in QCD and the renormalization properties of the Wilson loops. We consider the near forward elastic quark-quark scattering in the following kinematics:

$$s, m^2 \gg -t \gg \lambda^2 \gg \Lambda_{\text{QCD}}^2.$$

Here, $s = (p_1 + p_2)^2$ is the invariant energy of quarks with mass m , $t = (p_1 - p'_1)^2$ is the transferred momentum and λ^2 is the IR cutoff (characteristic hadronic scale) which is introduced to regularize infrared divergences. Notice that we don't need to fix the relation between s and m and quarks may be heavy. The scattering amplitude $T_{ij}^{i'j'}$ contains the color indices of the incoming and outgoing quarks. The quarks interact with each other by exchanging soft gluons with the total momentum $q = p_1 - p'_1$. In the center of mass frame of incoming quarks, for $s \gg -t$, the transferred momentum has the light-cone components $q = (q^+, q^-, \vec{q})$ with $q^\pm = \frac{1}{\sqrt{2}}(q^0 \pm q^3) = 0$ and $q^2 = -\vec{q}^2 = t$. Since the transferred momentum is much smaller than the energies of incoming quarks, the only effect of their interaction with soft gluons is

the appearance of additional phase in the wave functions of the incoming quarks. This phase, the so called eikonal phase, is equal to a Wilson line $P e^{i \int_C dx \cdot A(x)}$ defined in the fundamental representation of the $SU(N)$ group and evaluated along the classical trajectory C of the quark. We combine the eikonal phases of both quarks and obtain the representation for the quark-quark scattering amplitude as [11]

$$T_{ij}^{i'j'} \left(\frac{s}{m^2}, \frac{q^2}{\lambda^2} \right) = \sinh \gamma \int d^2 z e^{-i \vec{z} \cdot \vec{q}} W_{ij}^{i'j'}(\gamma, \vec{z}^2 \lambda^2), \quad t = -\vec{q}^2, \quad (2.2)$$

where the line function $W_{ij}^{i'j'}$ is given by

$$W_{ij}^{i'j'}(\gamma, \vec{z}^2 \lambda^2) = \langle 0 | T \left[P e^{ig \int_{-\infty}^{\infty} d\alpha v_1 \cdot A(v_1 \alpha)} \right]_{i'i} \left[P e^{ig \int_{-\infty}^{\infty} d\beta v_2 \cdot A(v_2 \beta + z)} \right]_{j'j} | 0 \rangle. \quad (2.3)$$

Here, two Wilson lines are evaluated along infinite lines in the direction of the quark velocities $v_1 = p_1/m$ and $v_2 = p_2/m$ and the integration paths are separated by the impact vector $z = (0^+, 0^-, \vec{z})$ in the transverse direction, $v_1 \cdot z = v_2 \cdot z = 0$.

Being expanded in powers of the gauge field, expression (2.2) reproduces the quark-quark scattering amplitude in the eikonal approximation. Integration over two-dimensional impact vector z was introduced in (2.2) to ensure the total transferred momentum in the t -channel to be $q = (0^+, 0^-, \vec{q})$. Indeed, it follows from (2.2) that the total momentum of gluons k_{tot} propagating in the t -channel is restricted by the following δ -functions:

$$\delta(k_{\text{tot}} \cdot v_1) \delta(k_{\text{tot}} \cdot v_2) \delta(\vec{k}_{\text{tot}} - \vec{q}) = \frac{1}{\sinh \gamma} \delta(k_{\text{tot}}^+) \delta(k_{\text{tot}}^-) \delta(\vec{k}_{\text{tot}} - \vec{q}) = \frac{1}{\sinh \gamma} \delta^{(4)}(k_{\text{tot}} - q),$$

where the first δ -function comes from integration over α in (2.3), the second one from integration over β and the last one from integration over \vec{z} in (2.2). To compensate the additional factor, $\sinh \gamma$, in the r.h.s. of this relation, the same factor was introduced in the expression (2.2).

The scattering amplitude (2.2) depends on the quark velocities v_1 and v_2 , the transferred momentum \vec{q} and IR cutoff λ . These variables give rise to only two scalar dimensionless invariants: $(v_1 v_2) = s/m^2$ and t/λ^2 as explicitly indicated in (2.2). The s -dependence of the amplitude comes through the dependence on the angle γ between quark 4-velocities v_1 and v_2 defined in Minkowski space-time as

$$(v_1 \cdot v_2) = \cosh \gamma. \quad (2.4)$$

For arbitrary velocities v_1 and v_2 , the angle γ may take real and complex values and in the limit of high energy quark-quark scattering ($s \gg m^2$) we have

$$\gamma = \log \frac{s}{m^2} \gg 1. \quad (2.5)$$

To find the asymptotic behavior of the scattering amplitude (2.2) one needs to know the vacuum expectation value of the Wilson lines (2.3). Let us consider first a special case of the elastic electron-electron scattering in QED.

2.1. High-energy scattering in QED

One may use the expression (2.2) for the scattering amplitude in this case, but the calculation of the Wilson line (2.3) is simplified because for abelian gauge group a path-ordered exponent coincides with an ordinary exponent. Moreover, since photons don't interact with each other, the calculation of Wilson lines in QED is reduced to the integration of a free photon propagator $D_{\mu\nu}(x)$ along the path and the result of calculation is

$$W_{\text{QED}}(\gamma, z^2 \lambda^2) = \exp\left(\frac{(ie)^2}{2} \int dx^\mu \int dy^\nu D_{\mu\nu}(x-y)\right) = (\lambda^2 \bar{z}^2 / 4)^{i\frac{e^2}{4\pi} \coth \gamma}, \quad (2.6)$$

where λ is a fictitious photon mass. After substitution of this relation into (2.2) and integration over impact vector we get the expression for the scattering amplitude in QED [14]

$$T_{\text{QED}}\left(\frac{s}{m^2}, \frac{t}{\lambda^2}\right) = ie^2 \frac{\cosh \gamma}{t} \left(\frac{-t}{\lambda^2}\right)^{-i\frac{e^2}{4\pi} \coth \gamma} \frac{\Gamma(1 + i\frac{e^2}{4\pi} \coth \gamma)}{\Gamma(1 - i\frac{e^2}{4\pi} \coth \gamma)}. \quad (2.7)$$

In the limit $s/m^2 \rightarrow \infty$ or, equivalently $\gamma \rightarrow \infty$, the expectation value (2.6) does not depend on s and, as a consequence, the scattering amplitude has the asymptotics $T/T_{\text{Born}} \sim s^0$ with $T_{\text{Born}} = \frac{ie^2}{t} \frac{s}{m^2}$ the amplitude in the Born approximation. This implies that photon is not reggeized in QED [14].

2.2. Wilson lines in perturbative QCD

The evaluation of the Wilson line in perturbative QCD is much more complicated than in QED. To explain the approach [11] for the evaluation of the Wilson line (2.3), let us consider as an example the one-loop calculation of W in the Feynman gauge. Using the definition (2.3), we get

$$W_{1\text{-loop}} = I \otimes I + (t^a \otimes t^a) \frac{g^2}{4\pi^{D/2}} \Gamma(D/2-1) \lambda^{4-D} \int_{-\infty}^{\infty} d\alpha \int_{-\infty}^{\infty} d\beta \frac{(v_1 v_2)}{[-(v_1 \alpha - v_2 \beta)^2 + \bar{z}^2 + i0]^{D/2-1}}, \quad (2.8)$$

where a direct product of the gauge generators defined in the fundamental representation takes care of the color indices of the quarks. In this expression, gluon is attached to both Wilson lines at points $v_1 \alpha$ and $v_2 \beta + z$ and we integrate the gluon propagator $v_1^\mu v_2^\nu D_{\mu\nu}(v_1 \alpha - v_2 \beta - z)$ over positions of these points. To regularize IR divergences we introduced the dimensional regularization with $D = 4 - 2\varepsilon$, ($\varepsilon < 0$) and λ being the IR renormalization parameter. There is another contribution to $W_{1\text{-loop}}$ corresponding to the case when gluon is attached by both ends to one of the Wilson lines. A careful treatment shows that this contribution vanishes. Performing integration over parameters α and β in (2.8) we get

$$W_{1\text{-loop}}(\gamma, \lambda^2 \bar{z}^2) = I \otimes I + (t^a \otimes t^a) \frac{\alpha_s}{\pi} (-i\pi \coth \gamma) \Gamma(-\varepsilon) (\pi \lambda^2 \bar{z}^2)^\varepsilon. \quad (2.9)$$

The integral over α and β in (2.8) has an infrared divergence coming from large α and β . In the dimensional regularization, this divergence appears in $W_{1\text{-loop}}$ as a pole in $(D-4)$ with the renormalization parameter λ having a sense of an IR cutoff. After renormalization in the $\overline{\text{MS}}$ -scheme, this result coincides up to color factor with the lowest term in the expansion of the analogous expression (2.6) in QED in powers of e^2 .

The evaluation of the Wilson line (2.3) in QCD is based on the following observation. The one-loop expression (2.9) for the line function is divergent for $\vec{z} = 0$ and $\varepsilon < 0$. This divergence has an ultraviolet origin because it comes from integration over small α and β in (2.8), that is from gluons propagating at short distances ($v_1\alpha - v_2\beta$) between quark trajectories as $\alpha, \beta \rightarrow 0$. One should notice that the ultraviolet (UV) divergences of Wilson lines at $z = 0$ have nothing to do with the “conventional” ultraviolet singularities in QCD. For $z = 0$, the integration paths of Wilson lines in (2.3) cross each other at point 0 and UV divergences, the so called cross divergences, appear when one integrates gluon propagators along integration path at the vicinity of the cross point [15]. We note that the cross divergences do not appear in $W_{1\text{-loop}}$ for nonzero z because, as it enters into the integral (2.8), nonzero \vec{z}^2 regularizes gluon propagator at short distances as $\alpha, \beta \rightarrow 0$.

Thus, \vec{z}^2 has a meaning of an UV cutoff for the one-loop line function W and the dependence of the original line function $W(\gamma, \lambda^2 \vec{z}^2)$ on z^2 is in one-to-one correspondence with the dependence of the same Wilson line but with $z = 0$ on the UV cutoff which we have to introduce to regularize the cross singularities. This property suggests the following way for calculation of the z -dependence of the Wilson lines (2.3). First, we put $z = 0$ in the definition (2.3) of the line function and introduce the regularization of cross singularities of W . Then, we renormalize cross singularities and identify UV cutoff with impact vector as $\mu^2 = 1/\vec{z}^2$. We conclude that the z -dependence of the line function W and, as consequence, the t -asymptotics of the scattering amplitude (2.2) are controlled by the renormalization properties of the cross singularities of Wilson loops.

2.3. Renormalization properties of Wilson lines

The renormalization properties of the loop functions in QCD have been studied in detail [15] and can be summarized as follows. Being expanded in powers of gauge potential, $W(C_1, \dots, C_n)$ can be expressed as multiple integrals of the Green functions along the paths $C_1 \dots C_n$. The loop function is not a well defined object because it contains different kinds of divergences. First of all, it has the conventional ultraviolet (UV) divergences of the Green functions in perturbative QCD. Moreover, as it was first found in [16], the Wilson loops have very specific UV divergences which depend on the properties of the integration paths C in the definition (2.3). For instance, the expansion of the loop function to the lowest order of PT involves the contour integral $\oint_C dx_\mu \oint_C dy_\nu D^{\mu\nu}(x - y)$ which is potentially divergent at $x = y$ due to singular behavior of the gluon propagator at short distances. The divergences come either when y approaches x along the path C or when the path crosses itself and both x and y approach the cross point. In both cases divergences have an UV origin because they come from integration at short distances. In the first case, UV divergences can be absorbed into renormalization of the coupling constant and gauge fields provided that the integration path is smooth everywhere. Otherwise, if the path is smooth everywhere except of a one point where it has a cusp, additional UV divergences, the so-called “cusp” singularities, appear which can be renormalized multiplicatively [17]. The corresponding anomalous dimension, $\Gamma_{\text{cusp}}(\gamma, g)$, the cusp anomalous dimension is a gauge invariant function of the coupling constant and the cusp angle. If the integration path crosses itself (or the paths $C_1 \dots C_n$ cross each other), additional “crossed” singularities appear in the loop function [15].

It was found [13] that these renormalization properties of the Wilson loops which look like their undesired features are of the most importance in perturbative QCD. The same function,

the cusp anomalous dimension of a Wilson line, appears when one studies the infrared (IR) singularities of on-shell form factors or the velocity-dependent anomalous dimension in the effective heavy quark field theory. The anomalous dimensions of the Wilson lines govern the IR logarithms in the same manner as the anomalous dimensions of the local composite twist-2 operators control the collinear singularities one encounters studying the structure functions of deep inelastic scattering. Moreover, there is a remarkable relation [11] between the high-energy behavior of the scattering amplitudes in the quasielastic unitarity approximation and the renormalization properties of the “cross” divergences of the loop function W .

2.4. Cross anomalous dimension

The renormalization properties of the cross divergences were studied in [15]. It was shown that the loop function (1.1) with all Wilson loops defined in the *fundamental* representation of the $SU(N)$ group ($R_1 = \dots = R_n = F$) and paths having a cross point, is mixed under renormalization with loop functions evaluated along the integration paths which are different from original paths at the vicinity of the cross point. As an important example we consider the Wilson lines $(W_1)_{ij}^{i'j'}$ and $(W_2)_{ij}^{i'j'}$ defined in fig.1. Although the integration paths in fig.1 have an infinite length and they are open we could get two Wilson loops by projecting the line functions $(W_1)_{ij}^{i'j'}$ and $(W_2)_{ij}^{i'j'}$ onto the color structure $\delta_{i'j}\delta_{j'i}$.

We choose the Wilson lines in fig.1(a) and 1(b) to be defined in the fundamental representation of the $SU(N)$ gauge group. According to the general analysis [15], the line function of fig.1(a) has cross singularities and under their renormalization it is mixed with the Wilson line of fig.1(b). As a consequence, the renormalized line functions W_1 and W_2 satisfy the following renormalization group (RG) equation [15]

$$\left(\mu \frac{\partial}{\partial \mu} + \beta(g) \frac{\partial}{\partial g} \right) W_a = -\Gamma_{\text{cross}}^{ab}(\gamma, g) W_b, \quad a, b = 1, 2, \quad (2.10)$$

where $W_a \equiv (W_a)_{ij}^{i'j'}$ and μ is renormalization point. Here, $\Gamma_{\text{cross}}(\gamma, g)$ is the cross anomalous dimension which is a gauge invariant 2×2 matrix depending only on the coupling constant and the angle γ between lines at the cross point. It is important to notice that the RG equation (2.10) is valid only in the fundamental representation of the gauge group and its generalization to another representations is unknown.

2.5. Evaluation of the scattering amplitude

We recall that the evaluation of the scattering amplitude (2.2) is based on the following property of the line function W . Using the definition (2.3) of W we introduce into consideration the Wilson line W_1 in fig.1(a). The only difference between them is that the integration paths in (2.3) do not cross each other for nonzero z . For $z \neq 0$ the Wilson line $W(\gamma, \bar{z}^2 \lambda^2)$ is UV finite but for $z = 0$ it coincides with W_1 and has cross divergences. The distance between quark trajectories, \bar{z}^2 , in the definition (2.3) of W plays a role of UV cutoff for cross singularities and the z -dependence of W is the same as the dependence of the Wilson line $W_1(\gamma, \mu^2/\lambda^2)$ on the renormalization parameter μ . Solving the RG equation (2.10) for $W_1(\gamma, \mu^2/\lambda^2)$ with the boundary conditions, $W_1(\gamma, 1) = \delta_{i'i}\delta_{j'j}$ and $W_2(\gamma, 1) = \delta_{i'j}\delta_{j'i}$, we substitute $\mu^2 = 1/\bar{z}^2$ and

find the following expression for the scattering amplitude [11]

$$T_{ij}^{i'j'}\left(\frac{s}{m^2}, \frac{\bar{q}^2}{\lambda^2}\right) = \sinh \gamma \int d^2 \vec{z} e^{-i\vec{z}\vec{q}} \left(A_{11}(\gamma, \vec{z}^2 \lambda^2) \delta_{ii'} \delta_{jj'} + A_{12}(\gamma, \vec{z}^2 \lambda^2) \delta_{ij'} \delta_{ji'} \right), \quad (2.11)$$

where A_{11} and A_{12} are elements of the 2×2 matrix

$$A_{\text{qq}}(\gamma, z^2 \lambda^2) = T \exp \left(- \int_{\lambda}^{1/z} \frac{d\tau}{\tau} \Gamma_{\text{cross}}(\gamma, g(\tau)) \right). \quad (2.12)$$

Notice, that the matrices $\Gamma_{\text{cross}}(\gamma, g(\tau))$ do not commute with each other for different values of τ and this makes difficult to evaluate the time-ordered exponent in (2.12). The expression (2.11) for the quark-quark scattering amplitude can be easily generalized to describe the quark-antiquark scattering. We notice that antiquark with a 4-velocity v_2 can be treated as a quark moving backward in time with velocity $-v_2$. As a result, to get the quark-antiquark scattering amplitude one has to replace one of the quark velocities $v_2 \rightarrow -v_2$ in expressions (2.11) and (2.12). Since the scattering amplitude (2.11) depends on the angle γ between velocities, this transformation corresponds to the replacement $\gamma \rightarrow i\pi - \gamma$ in the expression (2.12) for the matrix A , or equivalently in cross anomalous dimension:

$$A_{\text{q}\bar{\text{q}}}(\gamma, z^2 \lambda^2) = T \exp \left(- \int_{\lambda}^{1/z} \frac{d\tau}{\tau} \Gamma_{\text{cross}}(i\pi - \gamma, g(\tau)) \right),$$

where γ is the angle between velocities of incoming quark and antiquark.

The expression (2.11) takes into account all $\log t$ and $\log s$ corrections to the scattering amplitude. We conclude from (2.12) that it is the matrix of the cross anomalous dimensions which governs the high energy behavior of the scattering amplitude. As it follows from (2.11), the s -dependence of the amplitude comes from the γ -dependence of $\Gamma_{\text{cross}}(\gamma, g)$ while the t -dependence originates from the evolution of the coupling constant. To find the asymptotic behavior of the scattering amplitude (2.11) we need to know the large γ -behavior of $\Gamma_{\text{cross}}(\gamma, g)$ to all orders of perturbation theory. To this end, we perform the one-loop calculation of $\Gamma_{\text{cross}}(\gamma, g)$ in the next section and try to find the properties of this matrix which can be generalized to higher loop orders.

3. One-loop calculation of the cross anomalous dimension

To find the cross anomalous dimension we evaluate the line functions of fig.1(a) and 1(b) to the lowest order of PT and substitute them into (2.10). In the Born approximation the line functions have trivial expressions

$$W_1^{(0)} = \delta_{i'i} \delta_{j'j} \equiv |1\rangle, \quad W_2^{(0)} = \delta_{i'j} \delta_{j'i} \equiv |2\rangle, \quad (3.13)$$

where $|1\rangle$ and $|2\rangle$ denote two states in color space. To one-loop order the line functions are given by path integrals similar to that in (2.8). To evaluate the integrals we introduce the following parameterization of the integration paths of fig.1,

$$C_I = v_1 \alpha, \quad C_{II} = v_2 \beta, \quad C_{III} = v_1 \beta, \quad C_{IV} = v_2 \alpha, \quad (3.14)$$

where $0 < \alpha < \infty$ and $-\infty < \beta < 0$ and where v_1 and v_2 are quark velocities.

The integration paths in fig.1(a) and 1(b) cross each other at point 0 and go to infinity along the vectors v_1 and v_2 . As a consequence, the line functions W_1 and W_2 have UV divergences due to the cross point and IR divergences due to the infinite length of the paths. To regularize the cross singularities we use the dimensional regularization with $D = 4 - 2\varepsilon$ and in order to regularize IR divergences we introduce a fictitious gluon mass λ . We fix the Feynman gauge and define the gluon propagator in the coordinate representation as $D_{\mu\nu}(x) = g_{\mu\nu}D(x)$ with

$$D(x) = -i \int \frac{d^D k}{(2\pi)^D} \frac{e^{-ikx}}{k^2 - \lambda^2 + i0} = -\frac{1}{4\pi^{D/2}} \int_0^{-i\infty} d\alpha \alpha^{D/2-2} \exp\left(x^2\alpha - \frac{\lambda^2}{4\alpha}\right). \quad (3.15)$$

After the decomposition of the integration path of fig.1(a) as $C = C_I + C_{II} + C_{III} + C_{IV}$ we get the set of Feynman diagrams of fig.2 which contribute to one-loop corrections to the line function W_1 . Then, the contribution of the diagram of fig.2(1) to W_1 is given by

$$(ig)^2 t_{i'i}^a t_{j'j}^a \int_{C_I} dx_\mu \int_{C_{II}} dy_\nu D^{\mu\nu}(x-y) \equiv -g^2 (v_1 v_2) t^a \otimes t^a \int_0^\infty d\alpha \int_{-\infty}^0 d\beta D(v_1\alpha - v_2\beta),$$

where integration is performed over positions of gluons on the paths C_I and C_{II} and the direct product of the gauge group generators takes care of color indices of the line function. Substituting the gluon propagator (3.15) and integrating over α and β we get the expression for the ‘‘Feynman integral’’

$$F_1 = (ig)^2 \int_{C_I} dx_\mu \int_{C_{II}} dy_\nu D^{\mu\nu}(x-y) = -\frac{\alpha_s}{\pi} \left(\frac{4\pi\mu^2}{\lambda^2}\right)^\varepsilon \frac{\Gamma(1+\varepsilon)}{2\varepsilon} \gamma \coth \gamma. \quad (3.16)$$

Here, the cross singularity comes from the integration over small $x-y$ and it appears in the final expression as a pole in ε . Calculation of the remaining diagrams of fig.2 is analogous and gives the following results

$$F_2 = -\frac{\alpha_s}{\pi} \left(\frac{4\pi\mu^2}{\lambda^2}\right)^\varepsilon \frac{\Gamma(1+\varepsilon)}{2\varepsilon} (i\pi - \gamma) \coth \gamma, \quad F_3 = -2F_4 = -\frac{\alpha_s}{\pi} \left(\frac{4\pi\mu^2}{\lambda^2}\right)^\varepsilon \frac{\Gamma(1+\varepsilon)}{2\varepsilon}. \quad (3.17)$$

We notice that there are simple relations between these expressions: $F_2(\gamma) = -F_1(i\pi - \gamma)$, $F_3 = F_1(\gamma = 0)$. In Appendix A we explain their origin and show that analogous relations exist between two-loop Feynman integrals.

To evaluate the one-loop correction to the line function W_1 we take the expressions (3.16) and (3.17) and sum them with appropriate color and combinatoric factors:

$$W_1^{(1)} = t_{i'i}^a t_{j'j}^a (2F_1 + 2F_2) + C_F \delta_{i'i} \delta_{j'j} (2F_3 + 4F_4),$$

where $C_F = t^a t^a$ is the quadratic Casimir operator in the fundamental representation of the $SU(N)$ gauge group. This expression contains a pole in ε which is subtracted in the $\overline{\text{MS}}$ -scheme. Finally, the renormalized one-loop expression for the line function W_1 is given by

$$W_1^{(1)} = -\frac{\alpha_s}{\pi} \log \frac{\mu^2}{\lambda^2} (t_{i'i'}^a t_{j'j}^a) i\pi \coth \gamma. \quad (3.18)$$

The calculation of the line function W_2 involves the integration over the path of fig.1(b) which is different from the path of fig.1(a) only at the cross point. The contribution of the individual

Feynman diagram of fig.2 to the line function W_1 has the form of the product, $W = F \cdot C \cdot w$, of the corresponding Feynman integral (F), the color factor (C) and the combinatorial weight of the diagram (w). The difference between the paths of fig.1(a) and 1(b) at the cross point is not important when one calculates the Feynman integral F and the combinatorial weight w but it does affect the color factors of the corresponding diagrams. This means, that to any order of perturbation theory the same Feynman integrals contribute to both line functions and the only difference between W_1 and W_2 is that integrals enter with different color factors. In particular, using the expressions (3.16) and (3.17) we get the one-loop expression for the line function W_2 as

$$W_2^{(1)} = C_F \delta_{i'j} \delta_{j'i} (2F_1 + 4F_4) + t_{i'j}^a t_{j'i}^a (2F_2 + 2F_3).$$

After substitution of the Feynman integrals (3.16) and (3.17) into this expression we subtract a pole in the $\overline{\text{MS}}$ scheme and obtain the renormalized line function

$$W_2^{(1)} = \frac{\alpha_s}{\pi} \log \frac{\mu^2}{\lambda^2} \left[-C_F \delta_{i'j} \delta_{j'i} (\gamma \coth \gamma - 1) + t_{i'j}^a t_{j'i}^a (\gamma \coth \gamma - i\pi \coth \gamma - 1) \right]. \quad (3.19)$$

The obtained one-loop expressions (3.18) and (3.19) for the line functions are valid in an arbitrary representation of the $SU(N)$ group after proper redefinition of the Casimir operator C_F . The reason why the fundamental representation plays a special role comes from the fact that the direct product of the gauge group generators can be decomposed into the sum of invariant tensors

$$t_{ij}^a t_{kl}^a = -\frac{1}{2N} \delta_{ij} \delta_{kl} + \frac{1}{2} \delta_{il} \delta_{jk}. \quad (3.20)$$

After substitution of this decomposition into (3.18) and (3.19) we find that one-loop correction to W_1 contains a color structure of W_2 in the Born approximation, eq.(3.13), and vice versa. As a consequence, both line functions are mixed with each other under renormalization. In an arbitrary representation of the gauge group we do not have a relation similar to (3.20) and the renormalization properties of the line functions become complicated.

Substituting the one-loop results, (3.18) and (3.19), for the line functions into the RG equation (2.10) we find the one-loop expression for the matrix of cross anomalous dimension:

$$\Gamma_{\text{cross}}(\gamma, g) = \frac{\alpha_s}{\pi} \Gamma(\gamma), \quad (3.21)$$

$$\Gamma(\gamma) = \begin{pmatrix} -\frac{i\pi}{N} \coth \gamma & i\pi \coth \gamma \\ -\gamma \coth \gamma + 1 + i\pi \coth \gamma & N(\gamma \coth \gamma - 1) - \frac{i\pi}{N} \coth \gamma \end{pmatrix}.$$

Here, γ is the angle between quark velocities v_1 and v_2 in Minkowski space-time defined in (2.4).

3.1. Properties of the one-loop Γ_{cross}

The obtained expression (3.21) for one-loop Γ_{cross} obeys the following interesting properties. All elements of the matrix Γ_{cross} have nontrivial imaginary parts which change their sign under the replacement $\gamma \rightarrow i\pi - \gamma$:

$$\text{Im} \Gamma_{\text{cross}}(i\pi - \gamma, g) = -\text{Im} \Gamma_{\text{cross}}(\gamma, g).$$

As was shown in sect.2.5, this transformation of the angle allows us to relate quark-quark and quark-antiquark scattering amplitudes. Calculating the determinant of the matrix (3.21) we obtain the expression

$$\det \Gamma_{\text{cross}}(\gamma, g) = \left(\frac{\alpha_s}{\pi}\right)^2 \pi^2 \coth^2 \gamma \left(1 - \frac{1}{N^2}\right), \quad (3.22)$$

which, first, has zero imaginary part and, second, is invariant under $\gamma \rightarrow i\pi - \gamma$. This property implies that the elements of the matrix (3.21) are “fine tuned”. An additional argument in favour of this observation comes from the consideration of the large γ behavior of Γ_{cross} . In the limit of large γ different elements of the matrix have the following behavior

$$\Gamma_{\text{cross}}^{11} \sim \Gamma_{\text{cross}}^{12} \sim \mathcal{O}(\gamma^0), \quad \Gamma_{\text{cross}}^{12} \sim \Gamma_{\text{cross}}^{22} \sim \mathcal{O}(\gamma),$$

which leads to the asymptotics $\det \Gamma_{\text{cross}} \sim \mathcal{O}(\gamma)$ in general. However, the one-loop result (3.22) implies that the leading term $\mathcal{O}(\gamma)$ vanishes and the determinant has the asymptotics $\det \Gamma_{\text{cross}} \sim \mathcal{O}(\gamma^0)$ while $\text{tr} \Gamma_{\text{cross}} \sim \mathcal{O}(\gamma)$. The eigenvalues of the matrix $\Gamma(\gamma)$ satisfy the characteristic equation

$$\Gamma_{\pm}^2 - \Gamma_{\pm} \left(N\gamma \coth \gamma - N - \frac{2i\pi}{N} \coth \gamma \right) + (\pi \coth \gamma)^2 = 0. \quad (3.23)$$

Solving this equation we find that in the large γ limit both eigenvalues have positive real part ($\text{Re} \Gamma_{\pm} > 0$). Moreover, one of the eigenvalues of matrix Γ is much larger than the second one:

$$\begin{aligned} \Gamma_+ &= N\gamma - \left(N + \frac{2i\pi}{N} \right) - \pi^2 \frac{N^2 - 1}{N^3} \gamma^{-1} + \mathcal{O}(\gamma^{-2}), \\ \Gamma_- &= \pi^2 \frac{N^2 - 1}{N^3} \gamma^{-1} + \mathcal{O}(\gamma^{-2}), \end{aligned} \quad (3.24)$$

with $\gamma = \log(s/m^2)$ in the limit $s \gg m^2$.

3.2. Asymptotic behavior of the scattering amplitudes

Let us substitute the one-loop expression (3.21) for the matrix Γ_{cross} into (2.11) and (2.12). One-loop matrices $\Gamma_{\text{cross}}(\gamma, g(\tau))$ commute with each other for different τ and we can omit T -ordering in the definition (2.12) of the matrix A . After diagonalization of the one-loop matrix $\Gamma(\gamma)$ by a proper unitary transformation we get

$$A_{\text{qq}}(\gamma, \lambda^2 z^2) = \frac{\Gamma_+ - \Gamma(\gamma)}{\Gamma_+ - \Gamma_-} \exp\left(-\Gamma_- \int_{\lambda}^{1/z} \frac{d\tau}{\tau} \frac{\alpha_s(\tau)}{\pi}\right) + \frac{\Gamma_- - \Gamma(\gamma)}{\Gamma_- - \Gamma_+} \exp\left(-\Gamma_+ \int_{\lambda}^{1/z} \frac{d\tau}{\tau} \frac{\alpha_s(\tau)}{\pi}\right),$$

where the eigenvalues Γ_{\pm} were defined in (3.23). Finally, we find the following expression for the scattering amplitude (2.11)

$$T_{ij}^{i'j'} = \delta_{i'i} \delta_{j'j} T^{(0)} + t_{i'i}^a t_{j'j}^a T^{(8)}, \quad (3.25)$$

where two invariant amplitudes correspond to the exchange in the t -channel by states with the quantum numbers of vacuum and gluon and are given by

$$T^{(0)} = -\frac{\sinh \gamma}{t} \frac{\Gamma_+ \Gamma_-}{\Gamma_+ - \Gamma_-} (T_+ - T_-), \quad T^{(8)} = 2i\pi \frac{\cosh \gamma}{t} \frac{\Gamma_+ T_+ - \Gamma_- T_-}{\Gamma_+ - \Gamma_-}. \quad (3.26)$$

Here the notation was introduced for the Fourier transforms

$$T_{\pm} = \frac{t}{\Gamma_{\pm}} \int d^2z e^{-iz\cdot\bar{q}} \exp\left(-\Gamma_{\pm} \int_{\lambda}^{1/z} \frac{d\tau}{\tau} \frac{\alpha_s(\tau)}{\pi}\right). \quad (3.27)$$

Using one-loop expression for the coupling constant we get

$$T_{\pm} = \frac{t}{\Gamma_{\pm}} \int d^2z e^{-iz\cdot\bar{q}} \left(\frac{\log 1/z^2 \Lambda_{\text{QCD}}^2}{\log \lambda^2 / \Lambda_{\text{QCD}}^2}\right)^{-2\Gamma_{\pm}/\beta_0}. \quad (3.28)$$

Let us first consider the properties of the obtained expressions (3.26) and (3.27) in the leading $\log t$ approximation, $\alpha_s \log t / \lambda^2 \sim 1$. In this limit we may freeze the argument of the coupling constant in (3.27) and perform Fourier transformation to get

$$T_{\pm} = 2\alpha_s \exp\left(-\frac{\alpha_s}{2\pi} \Gamma_{\pm} \left(\frac{s}{m^2}\right) \log \frac{-t}{\lambda^2}\right) \frac{\Gamma\left(1 + \frac{\alpha_s}{2\pi} \Gamma_{\pm}\right)}{\Gamma\left(1 - \frac{\alpha_s}{2\pi} \Gamma_{\pm}\right)}. \quad (3.29)$$

This expression is similar to that (2.7) in QED and the only difference is that in QCD the s -dependence of the amplitudes is governed by the asymptotic behavior of the eigenvalues Γ_{\pm} . In the case of abelian gauge group the Wilson lines of figs.1(a) and 1(b) coincide and the cross anomalous dimension in QED is a c-number and not a matrix. As a result, the scattering amplitudes have different high energy behavior in QCD and QED.

Expanding (3.29) in powers of α_s we find that to the lowest order of PT

$$T_{\pm} = 2\alpha_s + \mathcal{O}(\alpha_s^2),$$

where higher order corrections involve $\log s$ and $\log t$ terms. After substitution of these values into (3.26) we recover the expressions for the scattering amplitude in the Born approximation

$$T^{(0)} = 0 + \mathcal{O}(\alpha_s^2), \quad T^{(8)} = \frac{ig^2}{t} \frac{s}{m^2} + \mathcal{O}(\alpha_s^2).$$

To find the behavior of the scattering amplitude (3.26) in the limit of high energies $s \gg m^2$, or equivalently for large cross angle (2.5), we start with the leading $\log t$ and $\log s$ approximation, $\alpha_s \log s / m^2 \log t / \lambda^2 \sim 1$. We use (3.24) and substitute $\Gamma_+ = N \log s / m^2$ and $\Gamma_- = 0$ into (3.29) and (3.26). The result has the standard reggeized form [18]:

$$T_{\text{LL}}^{(0)} = 0, \quad T_{\text{LL}}^{(8)} = T_{\text{Born}} \cdot \left(\frac{s}{m^2}\right)^{\alpha(t)}, \quad (3.30)$$

with the Regge trajectory $\alpha(t) = -\frac{\alpha_s}{2\pi} N \log \frac{-t}{\lambda^2}$. We can improve the leading logarithm approximation (3.30) by taking into account nonleading corrections to (3.29) in the limit $\alpha_s \log s / m^2 \sim \alpha_s \log t / \lambda^2 \sim 1$. Using the large energy behavior of the eigenvalues (3.24) we find the following expressions for the amplitudes of singlet and octet exchanges

$$T^{(0)} = -T_0 \Gamma_-(T_+ - T_-), \quad T^{(8)} = 2i\pi T_0 \left(T_+ - \frac{\Gamma_-}{\Gamma_+} T_-\right), \quad (3.31)$$

with $T_0 = \frac{s}{2m^2 t}$ and Γ_{\pm} defined in (3.24). The functions T_+ and T_- have a Regge like behavior (3.29) and for $\Gamma_+ \gg \Gamma_-$ we have $T_+ \ll T_-$. For $\Gamma_- = 0$ the expression (3.31) coincides with

the leading log result (3.30). We stress that the amplitude $T^{(0)}$ of the singlet exchange is unvanishing only due to nonleading logarithmic corrections. Moreover, as follows from (3.31), the amplitude $T^{(0)}$ gets dominant contribution from T_- and not from T_+ . The same is true for the amplitude $T^{(8)}$ of the octet exchange in which exponential fall of T_+ can not compete with the factor Γ_-/Γ_+ in front of T_- . Thus, the high-energy asymptotic behavior of the scattering amplitude (3.31) is dominated by the contribution of T_- and as a consequence the amplitude of the octet exchange is suppressed by the factor $1/\Gamma_+ = \mathcal{O}(\log^{-1} s/m^2)$ as compared to that to the amplitude of the singlet exchange. Comparing this behavior with (3.30) we conclude that nonleading logarithmic corrections drastically change the leading log asymptotics of the scattering amplitude.

Expression (3.29) was found under condition that we neglect the τ -dependence of the coupling constant $\alpha_s(\tau)$ in (3.27). We notice, however, that (3.29) becomes divergent for the special value of the coupling constant $\alpha_s = 2\pi/\Gamma_{\pm}$. To understand the origin of this divergence we deduce from (3.27) that it is the distance between quark trajectories, z^2 , which fixes the scale of the coupling constant. Then, for the perturbative expansion to be meaningful this distance should be much bigger than the QCD scale $1/\Lambda_{\text{QCD}}^2$. On the other hand, to get the scattering amplitude in (3.27) we have to integrate in (3.27) over all possible z^2 including large distances. For the z -integral in (3.27) to get dominant contribution in PT one has to impose additional conditions on Γ_{\pm} and \vec{q}^2 , or equivalently on s and t . Otherwise, the perturbative expression (3.27) become divergent at large distances. The analysis of PT applicability conditions for (3.27) can be performed similar to the analysis given in [19] for the Drell-Yan process.

The properties of the scattering amplitude are closely related to the particular form of the one-loop cross anomalous dimension (3.21). Natural question arises whether the asymptotic behavior of the scattering amplitudes will be changed after we take into account higher order corrections to the cross anomalous dimension. In the next section we answer this question by performing the calculation of the matrix of cross anomalous dimension to two-loop order in the Feynman gauge.

4. Two-loop calculation of the cross anomalous dimension

To find two-loop expression for the cross anomalous dimension we have to calculate the line functions W_1 and W_2 to the second order of PT by taking into account the next terms in the expansion of Wilson lines in powers of the coupling constant and effects of gluon self-interaction. The resulting Feynman diagrams contributing to W_1 are shown in figs.3–5 and we divide them into three different groups

1. QED-like diagrams of fig.3 in which gluons don't interact with each other;
2. Self-energy diagrams of fig.4 containing self-energy corrections to the gluon propagator;
3. Three-gluon diagrams of fig.5 having three-gluon vertex of self-interaction.

Evaluating the diagrams of fig.5 containing three gluon vertex, we notice that the Lorentz indices of the three gluon vertex $\Gamma^{\mu\nu\rho}$ are saturated by the vectors v_1 or v_2 depending to which line the gluons are attached. As a consequence, the diagrams with all three gluons attached to the same line vanish as $\Gamma_{\mu\nu\rho} v_1^\mu v_1^\nu v_1^\rho = 0$. We didn't include these diagrams in fig.5.

There many different Feynman integrals corresponding to the diagrams of figs.3–5 but, as we show in Appendix A, their calculation is reduced to the evaluation of only few “basic” diagrams after we take into account the properties of the Feynman integrals. The one-loop diagram of fig.2(1) and two-loop diagrams of fig.3(1)–(5), fig.4(1) and fig.5(1) form the set of the basic diagrams. Moreover, among them there are the diagrams which have been already calculated in [20].

4.1. Cusp anomalous dimension

As was shown in [20], the diagrams of fig.3(3)–(5), fig.4(1) and fig.5(1) contribute to the two-loop cusp anomalous dimension $\Gamma_{\text{cusp}}(\gamma, g)$ of Wilson loops. This anomalous dimension appears in the RG equation for the Wilson loop if the integration path has a cusp with the angle γ .

The fact that the same diagrams of fig.3(3)–(5), fig.4(1) and fig.5(1) contribute to the “cusp” and “cross” anomalous dimensions suggests that there might exist a relation between these two completely different functions of the angle γ . Indeed, the explicit form of this relation will be suggested in sect.5. Both anomalous dimensions depend on the representation of the $SU(N)$ in which the Wilson loop is defined. One might expect that if the relation between them does exist it contains Γ_{cross} and Γ_{cusp} taken in the same representation. In reality, as we will show in sect.5, the two-loop cross anomalous dimension calculated in the fundamental representation is related to the two-loop cusp anomalous dimension defined in the adjoint representation of the $SU(N)$.

The two-loop expression for $\Gamma_{\text{cusp}}(\gamma, g)$ in the adjoint representation of the $SU(N)$ is given by [20]

$$\Gamma_{\text{cusp}}(\gamma, g) = \frac{\alpha_s}{\pi} N(\gamma \coth \gamma - 1) + \left(\frac{\alpha_s}{\pi} N \right)^2 \Phi_{\text{cusp}}(\gamma), \quad (4.32)$$

where $\Phi_{\text{cusp}}(\gamma) = \Phi_{\text{QED}} + \Phi_{\text{self}} + \Phi_{3\text{-gluon}}$ and different kinds of the diagrams (QED-like of fig.3(3)–(5), self-energy of fig.4(1) and three-gluon of fig.5(1)) contribute to the corresponding functions:

$$\begin{aligned} \Phi_{\text{QED}}(\gamma) &= \coth^2 \gamma \int_0^\gamma d\psi \psi(\gamma - \psi) \coth \psi - \coth \gamma \int_0^\gamma d\psi \psi \coth \psi + \gamma \coth \gamma - \frac{1}{2}, \\ \Phi_{\text{self}}(\gamma) &= \frac{31}{36}(\gamma \coth \gamma - 1), \\ \Phi_{3\text{gluon}}(\gamma) &= -\frac{1}{2} \sinh(2\gamma) \int_0^\gamma d\psi \frac{\psi \coth \psi - 1}{\sinh^2 \gamma - \sinh^2 \psi} - \frac{\pi^2}{24}(\gamma \coth \gamma - 1). \end{aligned} \quad (4.33)$$

The properties of $\Gamma_{\text{cusp}}(\gamma, g)$ to higher orders of PT have been studied in [20].

4.2. QED like diagrams

The same QED-like diagrams of fig.3 contribute to the line functions W_1 and W_2 with different color and combinatorial factors. The explicit expressions for the color factors and the combinatorial weights are given in Appendix B.

To get the contribution of the QED-like diagrams of fig.3 to the line functions W_1 and W_2 we evaluate the corresponding Feynman integrals using the relations found in Appendix A, multiply them by color factors and combinatorial weights and sum the resulting expressions.

Finally, after lengthy calculation we get the following expression for the contribution of the diagrams of fig.3 to W_1

$$W_1^{\text{QED}} = \left(\frac{\alpha_s}{\pi}\right)^2 \log^2 \frac{\mu^2}{\lambda^2} \left[\left(-\frac{N^2+1}{8N^2} \pi^2 \coth^2 \gamma - \frac{i\pi}{8} \gamma \coth^2 \gamma + \frac{i\pi}{4} \coth \gamma \right) |1\rangle + \left(\frac{\pi^2}{4N} \coth^2 \gamma + \frac{i\pi}{8} N \gamma \coth^2 \gamma - \frac{i\pi}{4} N \coth \gamma \right) |2\rangle \right]. \quad (4.34)$$

We notice that this expression does not contain a single logarithm of μ . Although some individual diagrams do contain $\log(\mu^2/\lambda^2)$ -terms they cancel in the total sum of the diagrams. In terms of the RG equation (2.10), this means, that the QED-like diagrams don't contribute to the two-loop expressions for the elements Γ_{11} and Γ_{12} of the matrix of cross anomalous dimensions. The contribution of the QED-like diagrams to the line function W_2 can be found in analogous way. The resulting expression has the following structure:

$$W_2^{\text{QED}} = \left(\frac{\alpha_s}{\pi}\right)^2 \left(A_{\text{QED}} \log^2 \frac{\mu^2}{\lambda^2} + B_{\text{QED}} \log \frac{\mu^2}{\lambda^2} \right), \quad (4.35)$$

where in contrast with W_1^{QED} the coefficient B_{QED} in front of a single logarithm of μ is different from zero. The coefficient A_{QED} is given by

$$A_{\text{QED}} = \left\{ \left(\frac{\pi^2}{4N} + \frac{N^2+2}{8N} i\pi\gamma - \frac{1}{8} N\gamma^2 \right) \coth^2 \gamma + \left(-\frac{N^2+1}{4N} i\pi + \frac{3}{8} N\gamma \right) \coth \gamma - \frac{1}{4} N \right\} |1\rangle + \left\{ \left(-\frac{N^2+1}{8N^2} \pi^2 - \frac{3}{8} i\pi\gamma + \frac{1}{8} N^2 \gamma^2 \right) \coth^2 \gamma + \left(-\frac{3}{8} N^2 \gamma + \frac{i}{2} \pi \right) \coth \gamma + \frac{1}{4} N^2 \right\} |2\rangle.$$

The expression for the coefficient B_{QED} is complicated and it contains the integrals I_1 , I_2 and I_3 defined in (A.1). We simplify this expression using the identity (A.2) and after some algebra we recover the following relation between the coefficient B_{QED} and the function Φ_{QED} contributing to the two-loop cusp anomalous dimension (4.33):

$$B_{\text{QED}} = \frac{1}{2} N \Phi_{\text{QED}}(\gamma) [|1\rangle - N|2\rangle] - (\Phi_{\text{QED}}(\gamma) - \Phi_{\text{QED}}(i\pi - \gamma)) [N|1\rangle - |2\rangle]. \quad (4.36)$$

After substitution of the Wilson line (4.35) into the RG equation (2.10) we find that the coefficient B_{QED} contributes to the elements Γ_{21} and Γ_{22} of the matrix of the cross anomalous dimension. The identity (4.36) implies that the contribution of the QED-like diagrams to two different anomalous dimensions, Γ_{cross} and Γ_{cusp} , are closely related to each other.

4.3. Self-energy diagrams

Calculation of the self-energy diagrams of fig.4 to the Wilson lines can be easily done using the relations found in Appendix A. The total contribution of the diagrams of fig.4 to the line function W_1 is given by

$$W_1^{\text{self}} = \left(\frac{\alpha_s}{\pi}\right)^2 i\pi \coth \gamma \left(\frac{5}{48} \log^2 \frac{\mu^2}{\lambda^2} + \frac{31}{72} \log \frac{\mu^2}{\lambda^2} \right) (|1\rangle - N|2\rangle) \quad (4.37)$$

and it has the same color structure and the γ -dependence as the one-loop expression (3.18) for W_1 . For the total contribution of the self-energy diagrams to the line function W_2 we get

$$W_2^{\text{self}} = \left(\frac{\alpha_s}{\pi}\right)^2 \left(\frac{5}{48} \log^2 \frac{\mu^2}{\lambda^2} + \frac{31}{72} \log \frac{\mu^2}{\lambda^2} \right) \times \left[N(\gamma \coth \gamma - 1 - i\pi \coth \gamma) |1\rangle - \left(N^2(\gamma \coth \gamma - 1) - i\pi \coth \gamma \right) |2\rangle \right]. \quad (4.38)$$

Having the relation (4.36), it is tempting to find the analogous relation between the coefficient B_{self} in front of $\log(\mu^2/\lambda^2)$ in W_2^{self} and the function Φ_{self} defined in (4.33). It can be easily checked that the relation does exist and has the following form:

$$B_{\text{self}} = \frac{1}{2} N \Phi_{\text{self}}(\gamma) [|1\rangle - N|2\rangle] - \frac{1}{2} (\Phi_{\text{self}}(\gamma) - \Phi_{\text{self}}(i\pi - \gamma)) [N|1\rangle - |2\rangle]. \quad (4.39)$$

However, in contrast with B_{QED} , the second term in B_{self} has additional factor one-half.

4.4. Three-gluon diagrams

The diagrams of fig.5 contribute to the Wilson line W_1 with the same color factor defined in Appendix B. Then the identity (A.3) implies that the total contribution of the diagrams with three gluon vertex to the line function W_1 vanishes as

$$W_1^{3\text{gluon}} \propto F_1^{3\text{gluon}} + F_2^{3\text{gluon}} + F_3^{3\text{gluon}} = 0. \quad (4.40)$$

For the line function W_2 the color factors of the diagrams of fig.5 are different and their total contribution is unvanishing

$$W_2^{3\text{gluon}} = \left(\frac{\alpha_s}{\pi}\right)^2 \log \frac{\mu^2}{\lambda^2} B_{3\text{gluon}}, \quad (4.41)$$

where the coefficient $B_{3\text{gluon}}$ is given by

$$B_{3\text{gluon}} = \frac{1}{2} N \Phi_{3\text{gluon}}(\gamma) [|1\rangle - N|2\rangle] - (\Phi_{3\text{gluon}}(\gamma) - \Phi_{3\text{gluon}}(i\pi - \gamma)) [N|1\rangle - |2\rangle]. \quad (4.42)$$

We recognize that this relation between $B_{3\text{gluon}}$ and the contribution of three-gluon diagrams, $\Phi_{3\text{gluon}}$, to the cusp anomalous dimension is exactly the same as that for the QED-like diagrams in (4.36).

4.5. Two-loop cross anomalous dimension

Using the results of calculation of the Feynman diagrams of fig.3–5 we find the two-loop corrections to the line functions W_1 and W_2 as follows:

$$W_a^{(2)} = W_a^{\text{QED}} + W_a^{\text{self}} + W_a^{3\text{gluon}}, \quad (a = 1, 2),$$

where W_a^{QED} was defined in (4.34) and (4.35), W_a^{self} in (4.37) and (4.38) and $W_a^{3\text{gluon}}$ in (4.40) and (4.41). Recall, that the two-loop expressions for the Wilson lines

$$W_a = W_a^{(0)} + W_a^{(1)} + W_a^{(2)}, \quad (a = 1, 2),$$

should satisfy the RG equation (2.10). Here, $W_a^{(0)}$ is the Born terms defined in (3.13) and $W_a^{(1)}$ is the one-loop correction given by (3.18) and (3.19). As a nontrivial test of our calculations we find after cumbersome calculation that the two-loop Wilson lines W_1 and W_2 do obey the RG equation (2.10). Although the coefficients in front of $\log^2(\mu^2/\lambda^2)$ in the two-loop expressions for the diagrams of fig.3–5 are complicated, being combined together they give rise to the beta-function term in the RG equation (2.10) for W_a .

The RG equation (2.10) implies that the coefficients in front of $\log(\mu^2/\lambda^2)$ in the two-loop expression for the Wilson line $W_1^{(2)}$ contribute to the elements Γ_{11} and Γ_{12} of the matrix of cross anomalous dimensions Γ_{cross} and analogous coefficients in $W_2^{(2)}$ contribute to the elements Γ_{21} and Γ_{22} . Notice that W_1^{QED} and $W_1^{3\text{gluon}}$ do not contain $\log(\mu^2/\lambda^2)$ terms and the elements Γ_{11} and Γ_{12} get contribution only from the self-energy diagrams of fig.4. Using the expression (4.37) for W_1^{self} we get two-loop corrections to the elements of the matrix of cross anomalous dimension

$$\begin{aligned}\Gamma_{11}^{(2)}(\gamma, g) &= -\frac{31}{36}\left(\frac{\alpha_s}{\pi}\right)^2 i\pi \coth \gamma \\ \Gamma_{12}^{(2)}(\gamma, g) &= \frac{31}{36}\left(\frac{\alpha_s}{\pi}\right)^2 i\pi N \coth \gamma.\end{aligned}$$

These expressions differ from analogous one-loop expressions (3.21) only by the factor $\frac{\alpha_s}{\pi} N \frac{31}{36}$. Moreover, there is a simple relation between $\Gamma_{11}^{(2)}$ and $\Gamma_{12}^{(2)}$ and the two-loop contribution of the self-energy diagrams to the cusp anomalous dimension

$$\begin{aligned}\Gamma_{11}^{(2)}(\gamma, g) &= -\frac{1}{N^2}\left(\frac{\alpha_s}{\pi}N\right)^2 (\Phi_{\text{self}}(\gamma) - \Phi_{\text{self}}(i\pi - \gamma)) \\ \Gamma_{12}^{(2)}(\gamma, g) &= \frac{1}{N}\left(\frac{\alpha_s}{\pi}N\right)^2 (\Phi_{\text{self}}(\gamma) - \Phi_{\text{self}}(i\pi - \gamma)).\end{aligned}\tag{4.43}$$

Calculating two remaining elements, $\Gamma_{21}^{(2)}$ and $\Gamma_{22}^{(2)}$, we find that all three different kinds of the diagrams, W_2^{QED} , W_2^{self} and $W_2^{3\text{gluon}}$, contribute to them. Since the corresponding B -coefficients are related to the cusp anomalous dimension by the identities (4.36), (4.39) and (4.42), the final expression for the elements of the matrix of cross anomalous dimension can be represented as

$$\begin{aligned}\Gamma_{21}^{(2)} &= -\frac{1}{N}\left(\frac{\alpha_s}{\pi}N\right)^2 [\Phi_{\text{cusp}}(\gamma) - 2(\Phi_{\text{cusp}}(\gamma) - \Phi_{\text{cusp}}(i\pi - \gamma)) + (\Phi_{\text{self}}(\gamma) - \Phi_{\text{self}}(i\pi - \gamma))] \\ \Gamma_{22}^{(2)} &= \left(\frac{\alpha_s}{\pi}N\right)^2 \left[\Phi_{\text{cusp}}(\gamma) - \frac{2}{N^2}(\Phi_{\text{cusp}}(\gamma) - \Phi_{\text{cusp}}(i\pi - \gamma)) + \frac{1}{N^2}(\Phi_{\text{self}}(\gamma) - \Phi_{\text{self}}(i\pi - \gamma)) \right],\end{aligned}\tag{4.44}$$

where $\Phi_{\text{cusp}} = \Phi_{\text{QED}} + \Phi_{\text{self}} + \Phi_{3\text{gluon}}$ was defined in (4.33). The terms containing Φ_{self} appeared in the r.h.s. of these relations due to the additional one-half factor in the expression (4.39) for B_{self} . The terms containing $\Phi_{\text{cusp}}(\gamma)$ look like two-loop corrections to the cusp anomalous dimension (4.32) defined in the *adjoint* representation of the $SU(N)$.

5. Properties of the cross anomalous dimension

Having the explicit relations (4.43) and (4.44) between the two-loop corrections to $\Gamma_{\text{cross}}(\gamma, g)$ and $\Gamma_{\text{cusp}}(\gamma, g)$, we summarize our two-loop calculations by representing the matrix of cross

anomalous dimensions in the following form:

$$\begin{aligned}
\Gamma_{\text{cross}}^{11} &= -\frac{1}{N^2}\Gamma_1(\gamma, g) \\
\Gamma_{\text{cross}}^{12} &= \frac{1}{N}\Gamma_1(\gamma, g) \\
\Gamma_{\text{cross}}^{21} &= -\frac{1}{N}[\Gamma_{\text{cusp}}(\gamma, g) + \Gamma_1(\gamma, g) + \Gamma_2(\gamma, g)] \\
\Gamma_{\text{cross}}^{22} &= \Gamma_{\text{cusp}}(\gamma, g) + \frac{1}{N^2}[\Gamma_1(\gamma, g) + \Gamma_2(\gamma, g)],
\end{aligned} \tag{5.45}$$

where the notation was introduced

$$\begin{aligned}
\Gamma_1(\gamma, g) &= \left[\frac{\alpha_s}{\pi} N + \frac{31}{36} \left(\frac{\alpha_s}{\pi} N \right)^2 \right] i\pi \coth \gamma \\
\Gamma_2(\gamma, g) &= -2(\Gamma_{\text{cusp}}(\gamma, g) - \Gamma_{\text{cusp}}(i\pi - \gamma, g)).
\end{aligned} \tag{5.46}$$

We note, that the form of this expression was deduced from the properties of two-loop corrections (4.43) and (4.44) and it comes as a surprise that the one-loop expression (3.21) for $\Gamma_{\text{cross}}(\gamma, g)$ also obeys this relation. Interesting property of the obtained expression is that it expresses four originally independent elements of the matrix $\Gamma_{\text{cross}}(\gamma, g)$ in terms of only two functions, Γ_{cusp} and $\Gamma_1(\gamma, g)$. Written in this form, the relation (5.45) admits natural generalization to all orders of perturbation theory. Although we do not have a proof that (5.45) is valid to all orders of PT, we give below arguments in favour of (5.45).

Let us examine whether the properties of one-loop Γ_{cross} found in sect.2 are still valid after we take into account two-loop corrections in (5.45).

5.1. Imaginary part

The cusp anomalous dimension $\Gamma_{\text{cusp}}(\gamma, g)$ takes real positive values for real angles γ while $\Gamma_{\text{cusp}}(i\pi - \gamma, g)$ has a nontrivial imaginary part. It turns out that in the expression for the cross anomalous dimension (5.45), $\Gamma_1(\gamma, g)$ and $\Gamma_2(\gamma, g)$ have pure imaginary values and change sign under reflection $\gamma \rightarrow i\pi - \gamma$:

$$(\Gamma_a(\gamma, g))^\dagger = -\Gamma_a(\gamma, g), \quad \Gamma_a(i\pi - \gamma, g) = -\Gamma_a(\gamma, g), \quad (a = 1, 2).$$

This property is obvious for the function $\Gamma_1(\gamma, g)$ defined in (5.46). To prove it for the function $\Gamma_2(\gamma, g)$, we apply the following property of the cusp anomalous dimension

$$\begin{aligned}
2\Gamma_{\text{cusp}}(\gamma, g) &= \Gamma_{\text{cusp}}(i\pi - \gamma, g) + \Gamma_{\text{cusp}}(-i\pi - \gamma, g) \\
&= \Gamma_{\text{cusp}}(i\pi - \gamma, g) + [\Gamma_{\text{cusp}}(i\pi - \gamma, g)]^\dagger
\end{aligned}$$

which can be easily verified using (4.32).¹ As a result, the function $\Gamma_2(\gamma, g)$ can be expressed as

$$\begin{aligned}
\Gamma_2(\gamma, g) &= 2i \text{Im} \Gamma_{\text{cusp}}(i\pi - \gamma, g) = \Gamma_{\text{cusp}}(i\pi - \gamma, g) - \Gamma_{\text{cusp}}(-i\pi - \gamma, g) \\
&= \Gamma_{\text{cusp}}(i\pi - \gamma, g) - \Gamma_{\text{cusp}}(i\pi + \gamma, g)
\end{aligned}$$

¹In fact, the integrals I_1 , I_2 and I_3 defined in (A.1) satisfy analogous relation.

where in the last identity we used the fact that $\Gamma_{\text{cusp}}(\gamma, g)$ is an even function of the angle γ . Let us calculate the determinant of the matrix (5.45):

$$\det \Gamma_{\text{cross}}(\gamma, g) = \frac{N^2 - 1}{N^4} \Gamma_1(\gamma, g) (\Gamma_1(\gamma, g) + \Gamma_2(\gamma, g)).$$

We notice that Γ_{cusp} does not contribute to this expression due to special form of the matrix (5.45). Although the matrix Γ_{cross} is complex the determinant turns out to be real even function of the angle γ , since both Γ_1 and Γ_2 are imaginary odd functions of γ .

5.2. Large γ asymptotics

Let us consider the asymptotic behavior of the cross anomalous dimension for large angles γ between velocities v_1 and v_2 . We recall that γ is defined as an angle in Minkowski space-time and it may have arbitrary values. The large γ limit (2.5) corresponds to the high energy scattering of quarks with velocities v_1 and v_2 .

To find the asymptotics of the expression (5.45) for $\gamma \gg 1$ we need to know the analogous behavior of the functions $\Gamma_{\text{cusp}}(\gamma, g)$ and $\Gamma_{\text{cusp}}(i\pi - \gamma, g)$. To this end we study the most general situation and consider $\Gamma_{\text{cusp}}(\chi, g)$ with χ being the complex quantity with large (negative or positive) real part: $(\text{Re } \chi)^2 \gg 1$. After some algebra we get from the two-loop expression (4.32) for the cusp anomalous dimension that $\Gamma_{\text{cusp}}(\chi, g)$ is a linear function of χ in this limit,

$$\Gamma_{\text{cusp}}(\chi, g) = \chi \text{sign}(\text{Re } \chi) \Gamma_{\text{cusp}}(g) + \mathcal{O}((\text{Re } \chi)^0), \quad (5.47)$$

where the two-loop expression for the coefficient $\Gamma_{\text{cusp}}(g)$ is given by²

$$\Gamma_{\text{cusp}}(g) = \frac{\alpha_s}{\pi} N + \left(\frac{\alpha_s}{\pi} N \right)^2 \left(\frac{67}{36} - \frac{\pi^2}{12} \right).$$

Moreover, as was shown in [20], this asymptotic behavior is valid to all orders of PT. The higher order corrections to $\Gamma_{\text{cusp}}(\gamma, g)$ only modify the coefficient $\Gamma_{\text{cusp}}(g)$. Using the relations (5.47) and (5.46) we get the asymptotics of the function Γ_2 for large positive angles γ as

$$\Gamma_2(\gamma, g) = -2i\pi \Gamma_{\text{cusp}}(g) + \mathcal{O}(\gamma^{-1})$$

and the analogous expression for the function Γ_1 is

$$\Gamma_1(\gamma, g) = i\pi \Gamma_1(g) + \mathcal{O}(\gamma^{-1}), \quad \Gamma_1(g) = \frac{\alpha_s}{\pi} N + \frac{31}{36} \left(\frac{\alpha_s}{\pi} N \right)^2.$$

Thus, the large γ asymptotic behavior of the matrix of cross anomalous dimensions (5.45) is

$$\begin{aligned} \Gamma_{\text{cross}}^{11} &= -\frac{i\pi}{N^2} \Gamma_1(g) \\ \Gamma_{\text{cross}}^{12} &= \frac{i\pi}{N} \Gamma_1(g) \\ \Gamma_{\text{cross}}^{21} &= -\gamma \frac{1}{N} \Gamma_{\text{cusp}}(g) + \frac{i\pi}{N} (2\Gamma_{\text{cusp}}(g) - \Gamma_1(g)) \\ \Gamma_{\text{cross}}^{22} &= \gamma \Gamma_{\text{cusp}}(g) - \frac{i\pi}{N^2} (2\Gamma_{\text{cusp}}(g) - \Gamma_1(g)), \end{aligned} \quad (5.48)$$

²We recall, that Γ_{cusp} is defined in the adjoint representation of the $SU(N)$ group.

where we omitted nonleading in γ terms in real and imaginary parts of the matrix elements.

Let us calculate the eigenvalues Γ_{\pm} of the matrix $\Gamma_{\text{cross}}(\gamma, g)$. From (5.48) we find their sum as

$$\Gamma_+ + \Gamma_- = \text{tr} \Gamma_{\text{cross}}(\gamma, g) = \left(\gamma - \frac{2i\pi}{N^2} \right) \Gamma_{\text{cross}}(g)$$

and we may expect that both eigenvalues are of order γ . However, calculating the determinant of (5.48) we find the product of eigenvalues behaves as γ^0 ,

$$\Gamma_+ \Gamma_- = \det \Gamma_{\text{cross}}(\gamma, g) = \pi^2 \frac{N^2 - 1}{N^4} \Gamma_1(g) (2\Gamma_{\text{cusp}}(g) - \Gamma_1(g)).$$

This means that one of the eigenvalues is much larger than the second one: $\Gamma_+ = \mathcal{O}(\gamma)$ and $\Gamma_- = \mathcal{O}(\gamma^{-1})$. The explicit expressions for the eigenvalues are:

$$\begin{aligned} \Gamma_+ &= \left(\gamma - \frac{2i\pi}{N^2} \right) \Gamma_{\text{cusp}}(g) \\ \Gamma_- &= \left(\frac{1}{\gamma} + \frac{2i\pi}{N^2 \gamma^2} \right) \pi^2 \frac{N^2 - 1}{N^4} \frac{\Gamma_1(g) (2\Gamma_{\text{cusp}}(g) - \Gamma_1(g))}{\Gamma_{\text{cusp}}(g)}, \end{aligned} \quad (5.49)$$

where we omitted nonleading in γ terms in real and imaginary parts of these expressions.

To get some insight into the general structure of the matrix Γ_{cross} , let us study the large N limit defined as follows:

$$\alpha_s N = \text{fixed}, \quad N \rightarrow \infty.$$

We find from (4.32), (5.46) and (5.45) that the anomalous dimensions $\Gamma_{\text{cusp}}(\gamma, g)$, $\Gamma_1(\gamma, g)$ and $\Gamma_2(\gamma, g)$ survive in this limit. At the same time, all the elements of the matrix Γ_{cross} vanish except of the element Γ_{22} which becomes equal to the cusp anomalous dimension. As we show in Appendix C, this observation is valid to all loop order in PT and the elements of the matrix of cross anomalous dimension have the following large N behavior

$$\Gamma_{\text{cross}}^{11} = \mathcal{O}(N^{-2}), \quad \Gamma_{\text{cross}}^{12} = \mathcal{O}(N^{-1}), \quad \Gamma_{\text{cross}}^{21} = \mathcal{O}(N^{-1}), \quad \Gamma_{\text{cross}}^{22} = \Gamma_{\text{cusp}}(\gamma, g) + \mathcal{O}(N^{-2}), \quad (5.50)$$

where $\Gamma_{\text{cusp}}(\gamma, g)$ is defined in the adjoint representation of the $SU(N)$. We notice that the expression (5.45) for the cross anomalous dimension to higher orders of PT is consistent with large N behavior (5.50).

Summarizing our two-loop calculations we conclude that the higher order corrections to the matrix of anomalous dimensions are organized in such a way, that they preserve the asymptotic behavior of the eigenvalues (5.49). This allows us to apply the results of sect.3.2 and find the higher energy behavior of the scattering amplitudes in QCD.

6. Conclusions

In this paper we considered the elastic quark-quark scattering at high energy s and fixed transferred momentum t . We have shown that all effects of interaction of incoming quarks with soft gluons are factorized into Wilson lines which appear as eikonal phases of the scattering quarks. As a consequence, the quark-quark scattering amplitude is represented as an expectation value of a Fourier transformed Wilson line evaluated along the integration path which consists of two semiclassical quark trajectories separated by the impact parameter in the transverse direction.

We evaluated the scattering amplitude using the fact that for zero impact parameter the Wilson line has additional cross singularities. We have shown that the asymptotic behavior of the scattering amplitude is governed by the matrix of cross anomalous dimension $\Gamma_{\text{cross}}(\gamma, g)$ which depends on the energy of incoming quarks through the angle γ between quark velocities. We performed two-loop calculation of $\Gamma_{\text{cross}}(\gamma, g)$ and found remarkable properties of this matrix. It turned out that four originally independent elements of $\Gamma_{\text{cross}}(\gamma, g)$ can be expressed in terms of only two functions, the cusp anomalous dimension $\Gamma_{\text{cusp}}(\gamma, g)$ and $\Gamma_1(\gamma, g)$ which comes from self-energy diagrams. Written in this form, the elements of $\Gamma_{\text{cross}}(\gamma, g)$ admit natural generalization to higher orders of PT. The form of the corresponding expressions was confirmed by the large N analysis of the Wilson lines. Higher order corrections are organized in such a way that they preserve the asymptotic behavior of the eigenvalues of the matrix of cross anomalous dimension. This allowed us to apply the one-loop result for $\Gamma_{\text{cross}}(\gamma, g)$ to find the high energy asymptotic of the quark-quark scattering amplitude. This amplitude can be decomposed into singlet and octet invariant amplitudes corresponding to the exchange in the t -channel with quantum numbers of vacuum and gluon, respectively. To any order of PT theory the octet amplitude gets large double logarithmic corrections while corrections to the singlet amplitude are nonleading. However, after resummation to all orders of PT these large corrections are summed into the exponentially small Sudakov like exponent with the slope depending on the eigenvalues of the matrix of cross anomalous dimensions. As a result, with leading and non-leading logarithmic corrections taken into account, the singlet amplitude dominates in the high energy asymptotic behavior of the quark-quark scattering amplitude.

Acknowledgements

We are grateful for helpful conversations with J. De Boer, G. Marchesini, G. Sterman and A. Radyushkin. This work was supported in part by the National Science Foundation under grant PHY9309888.

Appendix A. Basic diagrams

Let us consider the diagram of fig.3(1). Using the parameterization of the integration path (3.14) we find the following expression for the Feynman integral:

$$F_1^{\text{QED}} = (ig)^4 (v_1 v_2)^2 \int_0^\infty d\alpha_1 \int_0^{\alpha_1} d\alpha_2 \int_0^\infty d\alpha_3 \int_{-\infty}^0 d\beta D(v_1 \alpha_1 - v_2 \beta) D(v_1 \alpha_2 - v_2 \alpha_3),$$

where the D -function was defined in (3.15). It is convenient to introduce the following integrals:

$$\begin{aligned} I_1(\gamma) &= \int_0^\gamma d\psi \psi \coth \psi \\ I_2(\gamma) &= \int_0^\gamma d\psi \psi (\gamma - \psi) \coth \psi \\ I_3(\gamma) &= \int_0^\gamma d\psi \frac{\psi \coth \psi - 1}{\sinh^2 \gamma - \sinh^2 \psi} \log \frac{\sinh \gamma}{\sinh \psi}. \end{aligned} \tag{A.1}$$

Thus defined functions obey the following property

$$I_2(i\pi - \gamma) + \gamma I_1(i\pi - \gamma) = I_2(\gamma) + (i\pi - \gamma) I_1(\gamma). \tag{A.2}$$

Then the final expression for the Feynman integral looks like

$$F_1^{\text{QED}}(\gamma) = \frac{1}{4} \left(\frac{\alpha_s}{\pi} \right)^2 \left(\frac{4\pi\mu^2}{\lambda^2} \right)^{2\varepsilon} \Gamma(2\varepsilon) \coth^2 \gamma \\ \times \left(\frac{\Gamma(1+\varepsilon)\Gamma(\varepsilon)}{\Gamma(1+2\varepsilon)} \gamma(i\pi - \gamma) + 2\gamma I_1(i\pi - \gamma) - 2(i\pi - \gamma)I_1(\gamma) \right).$$

The cross singularities appear in F_1 as a double pole in ε . However, the diagram contains a divergent subgraph and in order to renormalize F_1 we have to subtract the cross divergence of this subgraph from F_1 . The corresponding counter term is proportional in the $\overline{\text{MS}}$ -scheme to the one-loop expression (3.16)

$$[F_1^{\text{QED}}(\gamma)]_{c.-t.} = - \left(\frac{\alpha_s}{\pi} \right)^2 \left(\frac{4\pi\mu^2}{\lambda^2} \right)^\varepsilon \frac{\Gamma(1+\varepsilon)}{4\varepsilon^2} \gamma(i\pi - \gamma) \coth^2 \gamma.$$

To renormalize the contribution of the diagram we add $[F_1^{\text{QED}}]_{c.-t.}$ to F_1^{QED} and subtract poles from the sum in the $\overline{\text{MS}}$ -scheme to find the following renormalized expression

$$F_1^{\text{QED}}(\gamma) = \left(\frac{\alpha_s}{\pi} \right)^2 \coth^2 \gamma \left\{ \frac{1}{8} \gamma(i\pi - \gamma) \log^2 \frac{\mu^2}{\lambda^2} + \frac{1}{2} [\gamma I_1(i\pi - \gamma) - (i\pi - \gamma)I_1(\gamma)] \log \frac{\mu^2}{\lambda^2} \right\}.$$

The calculation of the diagram of fig.3(2) is analogous to that of F_1^{QED} and the final renormalized expression for the diagram is

$$F_2^{\text{QED}}(\gamma) = \left(\frac{\alpha_s}{\pi} \right)^2 \coth \gamma \left\{ \frac{1}{8} \gamma \log^2 \frac{\mu^2}{\lambda^2} + \frac{1}{2} [I_1(\gamma) - \gamma] \log \frac{\mu^2}{\lambda^2} \right\}$$

where the corresponding counter term was taking into account.

Cusp anomalous dimension

The diagrams of fig.3(3)-(5), fig.4(1) and fig.5(1) have been already calculated in [20]. Using the results of the paper [20] we get the following renormalized expressions for the diagram of fig.3(3)

$$F_3^{\text{QED}} = \left(\frac{\alpha_s}{\pi} \right)^2 I_2(\gamma) \coth^2 \gamma \log \frac{\mu^2}{\lambda^2},$$

where the integral I_2 was defined in (A.1). For the diagram of fig.3(4) we have

$$F_4^{\text{QED}} = \left(\frac{\alpha_s}{\pi} \right)^2 \coth \gamma \left\{ \frac{1}{8} \gamma \log^2 \frac{\mu^2}{\lambda^2} + \frac{1}{2} [\gamma - I_1(\gamma)] \log \frac{\mu^2}{\lambda^2} \right\},$$

for the diagram of fig.3(5) we get

$$F_5^{\text{QED}} = \left(\frac{\alpha_s}{\pi} \right)^2 \coth^2 \gamma \left[\frac{1}{8} \gamma^2 \log^2 \frac{\mu^2}{\lambda^2} - I_2(\gamma) \log \frac{\mu^2}{\lambda^2} \right],$$

for the diagram of fig.4(1) containing self-energy correction to the gluon propagator

$$F_1^{\text{self}} = - \left(\frac{\alpha_s}{\pi} \right)^2 \left(\frac{5}{48} \log^2 \frac{\mu^2}{\lambda^2} + \frac{31}{72} \log \frac{\mu^2}{\lambda^2} \right) \gamma \coth \gamma,$$

for the diagram of fig.5(1)

$$F_1^{3\text{gluon}} = \left(\frac{\alpha_s}{\pi}\right)^2 \left[\frac{\pi^2}{96}(\gamma \coth \gamma - 1) + \frac{1}{8}I_3(\gamma) \sinh(2\gamma) \right] \log \frac{\mu^2}{\lambda^2}.$$

As was shown in [20], all these diagrams contribute to the two-loop cusp anomalous dimension.

Ward identities

The Feynman diagrams of figs.3(7) and 3(4) can be interpreted as propagator and vertex corrections to the one-loop diagram of fig.2(1). As was shown in [20], there are the Ward identities for the Wilson lines, analogous to the Ward identities between Green functions in QCD, which relate these two diagrams as follows:

$$F_7^{\text{QED}} = -F_4^{\text{QED}}.$$

The same identity is valid for the diagrams of figs.4(8) and 4(7):

$$F_8^{\text{QED}} = -F_7^{\text{QED}} = F_4^{\text{QED}},$$

and for the diagrams of figs.5(2) and 5(1):

$$F_2^{\text{self}} = -\frac{1}{2}F_1^{\text{self}}(0),$$

where the factor one-half takes into account that the self-energy correction is a ‘‘square root’’ of the propagator and $F_1^{\text{self}}(0)$ means the value of the Feynman integral F_1^{self} evaluated at $\gamma = 0$.

Reflection symmetry: $\gamma \rightarrow i\pi - \gamma$

The integration paths in figs.1(a) and 1(b) are defined by two vectors v_1 and v_2 in Minkowski space-time. Let us consider the properties of the diagrams under the reflection $v_2 \rightarrow -v_2$ or in terms of the angle between vectors $\gamma \rightarrow i\pi - \gamma$. Under this transformation the integration path transforms into itself but the orientation of the v_2 -line becomes opposite to the original one. After inverting of the direction of integration along v_2 -line as $\int_a^b dx A(x) = -\int_b^a dx A(x)$ we get formally another diagram multiplied by the factor $(-)^{\#}$ with $\#$ being the number of gluons attached to the v_2 -line. Thus, taking one of the diagrams of fig.3, we change the angle in the corresponding Feynman integral as $\gamma \rightarrow i\pi - \gamma$ and multiply the result by appropriate $(-)^{\#}$ to get the Feynman integral corresponding to another diagram. As a result, we find the following useful relations between the Feynman integrals of QED like diagrams

$$\begin{aligned} F_9^{\text{QED}} &= F_3^{\text{QED}}(i\pi - \gamma), & F_{10}^{\text{QED}} &= -F_4^{\text{QED}}(i\pi - \gamma), & F_{11}^{\text{QED}} &= F_5^{\text{QED}}(i\pi - \gamma) \\ F_{12}^{\text{QED}} &= -F_7^{\text{QED}}(i\pi - \gamma) = F_4^{\text{QED}}(i\pi - \gamma), & F_{13}^{\text{QED}} &= F_1^{\text{QED}}(i\pi - \gamma) \\ F_{14}^{\text{QED}} &= -F_8^{\text{QED}}(i\pi - \gamma) = -F_4^{\text{QED}}(i\pi - \gamma), & F_{15}^{\text{QED}} &= -F_2^{\text{QED}}(i\pi - \gamma), \end{aligned}$$

and between self-energy and three gluon diagrams

$$F_3^{\text{self}} = -F_1^{\text{self}}(i\pi - \gamma), \quad F_2^{3\text{gluon}} = -F_1^{3\text{gluon}}(i\pi - \gamma).$$

Notice that we don't have the same relations between the color factors of the diagrams, because after inverting the direction of the integration along v_2 -line the color indices of the gauge fields $A_\mu(x) = A_\mu^a(x)t^a$ become anti-path-ordered along the v_2 -line.

$\gamma \rightarrow 0$ limit

Let us consider the diagram of fig.3(16) in which all gluons are attached to only one of the lines. A simple observation is that the Feynman integral of this diagram can be obtained from the Feynman integral of the diagram of fig.3(3) in the limit $v_1 \rightarrow v_2$ or in terms of the angle $\gamma \rightarrow 0$. The same property leads to the following relations between QED like diagrams:

$$F_{16}^{\text{QED}} = F_3^{\text{QED}}(0), \quad F_{17}^{\text{QED}} = F_4^{\text{QED}}(0), \quad F_{18}^{\text{QED}} = F_5^{\text{QED}}(0), \quad F_{19}^{\text{QED}} = F_7^{\text{QED}}(0)$$

and between self-energy diagrams

$$F_4^{\text{self}} = F_1^{\text{self}}(0),$$

where in the r.h.s. the corresponding Feynman integrals are evaluated at $\gamma = 0$.

Factorization

We notice, that in the Feynman diagram of fig.3(20) two gluon propagator are independently integrated along the path. As a consequence, the corresponding Feynman integral can be factorized into the product of two independent one-loop integrals which have been calculated in sect.2. The same factorization property leads to the following relations:

$$F_{20}^{\text{QED}} = (F_2^{1\text{-loop}})^2, \quad F_{21}^{\text{QED}} = (F_1^{1\text{-loop}})^2, \quad F_{22}^{\text{QED}} = F_{23}^{\text{QED}} = F_1^{1\text{-loop}} F_4^{1\text{-loop}}$$

$$F_{24}^{\text{QED}} = F_{25}^{\text{QED}} = F_2^{1\text{-loop}} F_4^{1\text{-loop}}, \quad F_{26}^{\text{QED}} = F_{27}^{\text{QED}} = F_1^{1\text{-loop}} F_3^{1\text{-loop}}, \quad F_{28}^{\text{QED}} = (F_3^{1\text{-loop}})^2.$$

Using the expressions for the basic Feynman integrals and applying all these relations we can find the Feynman integrals for all the diagrams of figs.3–5 except of that for the diagram of fig.5(3). The calculation of the diagram of fig.5(3) is based on the following property. It turns out that the sum of the Feynman integrals corresponding to the diagrams of figs.5(1)–(3) vanishes, that is

$$F_3^{\text{3gluon}} = -F_1^{\text{3gluon}} - F_2^{\text{3gluon}} = -F_1^{\text{3gluon}}(\gamma) + F_1^{\text{3gluon}}(i\pi - \gamma). \quad (\text{A.3})$$

To show this we notice that three diagrams of fig.5 correspond to all possible positions of two gluons on one of the lines provided that the gluons are ordered with respect to each other. Moreover, applying the reflection symmetry we may extend the integration over position of third gluon from $[0, \infty)$ to $(-\infty, \infty)$ and take one-half of the result. The calculation of the Feynman integrals is more simple in the momentum space. Let us denote the momenta of gluons as k_a , $a = 1, 2, 3$ with $k_1 + k_2 + k_3 = 0$ and k_3 being the momentum of a single gluon attached to the v_2 line. Then, taking into account the expression for three-gluon vertex, we get the following momentum integral for the sum of the diagrams of fig.5(1)–(3),

$$\propto (v_1^2 v_2^\mu - (v_1 \cdot v_2) v_1^\mu) \int \frac{d^D k_3}{k_3^2} \delta(k_3 \cdot v_1) \delta(k_3 \cdot v_2) \int \frac{d^D k_1}{k_1^2} \frac{k_1^\mu}{(k_1 + k_3)^2 (k_1 \cdot v_1)}$$

where two delta functions appear after integration over positions of gluons on v_1 and v_2 lines from $-\infty$ to ∞ . The momentum integral is proportional to the only vector involved, v_1^μ , while the prefactor is orthogonal to v_1 . The product is zero which means that the sum of the Feynman integrals corresponding to the diagrams of fig.5(1)–(3) vanishes.

Appendix B. Color factors and combinatorial weights

The relation (3.20) implies that the color factors for the diagrams of fig.3–5 have the following general form

$$C = C_1 \delta_{ii'} \delta_{jj'} + C_2 \delta_{ij'} \delta_{ji'} = C_1 |1\rangle + C_2 |2\rangle, \quad (\text{B.1})$$

where the coefficients C_1 and C_2 are different for the same diagram contributing to W_1 and W_2 . Recall, that the relations (3.20) and (B.1) are unique properties of the fundamental representation of the $SU(N)$ group.

QED like diagrams

The general form of the color factors is given by (B.1) in the fundamental representation of the $SU(N)$. Consider, as an example, calculation of the color factor of the diagram of fig.3(1). This diagram contributes to the both line functions, W_1 and W_2 , with the color factors C_1^1 and C_1^2 , respectively, given by

$$\begin{aligned} C_1^1 &= (t^a t^b)_{i'i} (t^b t^a)_{j'j} = \frac{1}{4N^2} |1\rangle + \frac{N^2 - 2}{4N} |2\rangle \\ C_1^2 &= (t^a t^b t^a)_{i'j} t_{j'i}^a = -\frac{1}{4N} |1\rangle + \frac{1}{4N^2} |2\rangle, \end{aligned}$$

where we substituted the identity (3.20) and the states $|1\rangle$ and $|2\rangle$ were defined in (3.13). The calculation of the color factors of the remaining QED like diagrams of fig.3 is analogous. The calculation of the color factors of the QED like diagrams of fig.3 leads to the following expressions

$$\begin{aligned} C_2^1 &= C_4^1 = C_{10}^1 = C_{15}^1 = \frac{1}{4N^2} |1\rangle - \frac{1}{4N} |2\rangle \\ C_3^1 &= C_{11}^1 = C_{13}^1 = C_{20}^1 = \frac{N^2 + 1}{4N^2} |1\rangle - \frac{1}{2N} |2\rangle \\ C_7^1 &= C_8^1 = C_{12}^1 = C_{14}^1 = C_{22}^1 = C_{23}^1 = C_{24}^1 = C_{25}^1 = -\frac{N^2 - 1}{4N^2} |1\rangle + \frac{N^2 - 1}{4N} |2\rangle \\ C_{16}^1 &= C_{17}^1 = C_{18}^1 = C_{19}^1 = C_{26}^1 = C_{27}^1 = C_{28}^1 = -\frac{N^2 - 1}{4N^2} |1\rangle \\ C_6^1 &= N |1\rangle, \quad C_5^1 = C_{21}^1 = \frac{1}{4N^2} |1\rangle + \frac{N^2 - 2}{4N} |2\rangle, \end{aligned}$$

where the lower index numerates the diagrams of fig.3 and the upper index is related to the Wilson line W_1 . The color factors of the diagrams contributing to the Wilson line W_2 are

$$\begin{aligned} C_2^2 &= C_{12}^2 = C_{13}^2 = C_{19}^2 = C_{24}^2 = C_{25}^2 = C_{26}^2 = C_{27}^2 = \frac{N^2 - 1}{4N} |1\rangle - \frac{N^2 - 1}{4N^2} |2\rangle \\ C_3^2 &= C_4^2 = C_5^2 = C_6^2 = C_7^2 = C_{21}^2 = C_{22}^2 = C_{23}^2 = -\frac{N^2 - 1}{4N^2} |2\rangle \\ C_8^2 &= C_{10}^2 = C_{17}^2 = -\frac{1}{4N} |1\rangle + \frac{1}{4N^2} |2\rangle \end{aligned}$$

$$C_9 = C_{15} = C_{18} = C_{28} = \frac{N^2 - 2}{4N}|1\rangle + \frac{1}{4N^2}|2\rangle$$

$$C_{11}^2 = C_{14}^2 = C_{16}^2 = C_{20}^2 = -\frac{1}{2N}|1\rangle + \frac{N^2 + 1}{4N^2}|2\rangle.$$

The combinatorial weight of the QED like diagrams are given by

$$w_3 = w_5 = w_9 = w_{11} = w_{16} = w_{18} = 2, \quad w_{20} = w_{21} = w_{28} = 1$$

and the combinatorial weight of the remaining diagrams of fig.3 is equal to 4.

Self-energy diagrams

The color factors of the self-energy diagrams of fig.4 are defined as follows:

$$C_1^1 = C_3^1 = -\frac{1}{2}|1\rangle + \frac{N}{2}|2\rangle, \quad C_2^1 = C_4^1 = \frac{N^2 - 1}{2}|1\rangle$$

$$C_1^2 = C_2^2 = \frac{N^2 - 1}{2}|2\rangle, \quad C_3^2 = C_4^2 = \frac{N}{2}|1\rangle - \frac{1}{2}|2\rangle$$

and the combinatorial weights of the diagrams are

$$w_1 = w_3 = w_4 = 2, \quad w_2 = 4.$$

Three-gluon diagrams

The diagrams of fig.5 contribute to the line function W_1 with the color factors

$$C_1^1 = C_2^1 = C_3^1 = -2if^{abc}(t^a t^b)_{i'i} t_{j'j}^c = -\frac{1}{2}|1\rangle + \frac{N}{2}|2\rangle,$$

where f^{abc} are structure constants of the $SU(N)$ and the combinatorial weights are

$$w_1 = w_2 = w_3 = 4.$$

For the line function W_2 combinatorial weights are the same but the color factors of the diagrams of fig.5 are different

$$C_1^2 = \frac{N^2 - 1}{2}|2\rangle, \quad C_2^2 = -C_3^2 = \frac{N}{2}|1\rangle - \frac{1}{2}|2\rangle.$$

Appendix C. Large N limit of the cross anomalous dimension

To find relations (5.50) we consider the RG equation (2.10) for the Wilson lines W_a and multiply the both sides of the equation by $\delta_{i'i}\delta_{j'j}$. After contracting of the color indices we get from W_1 and W_2 two Wilson loops which are closed at infinity and have the following large N normalization

$$(W_1)_{ij}^{i'j'} \delta_{i'i} \delta_{j'j} = N^2 w_1, \quad (W_2)_{ij}^{i'j'} \delta_{i'i} \delta_{j'j} = N w_2, \quad (\text{C.1})$$

with $w_a = \mathcal{O}(N^0)$ and $a = 1, 2$. We notice, that such defined w_1 is given by the vacuum averaged product of two “elementary” Wilson loops calculated along v_1 and v_2 lines. The simplification of w_1 appears in the large N limit after we will take into account the following factorization property (vacuum dominance) [12]

$$\langle 0|\mathcal{O}_1\mathcal{O}_2|0\rangle = \langle 0|\mathcal{O}_1|0\rangle\langle 0|\mathcal{O}_2|0\rangle \times (1 + \mathcal{O}(N^{-2}))$$

valid for two arbitrary gauge invariant operators \mathcal{O}_1 and \mathcal{O}_2 . In our case, \mathcal{O}_1 is given by $P \exp(ig \int_{-\infty}^{\infty} ds v_1 A(v_1 s))$ and the expression for \mathcal{O}_2 is analogous with replacement v_1 by v_2 . As a result, the Wilson loop w_1 has a trivial value

$$w_1 = 1 + \mathcal{O}(N^{-2}). \quad (\text{C.2})$$

since $\langle 0|\mathcal{O}_1|0\rangle = \langle 0|\mathcal{O}_2|0\rangle = 1$. Notice, that the first nonleading correction to w_1 behaves as $\mathcal{O}(N^{-2})$ and not like $\mathcal{O}(N^{-1})$.

After substitution of (C.1) and (C.2) into the RG equation (2.10) we find the following identity in the large N limit

$$\Gamma_{\text{cross}}^{11} + \frac{1}{N}\Gamma_{\text{cross}}^{12}w_2 = \mathcal{O}(N^{-2}).$$

The requirement that the both terms in the l.h.s. of this relation have the same large N behavior leads together with $w_2 = \mathcal{O}(N^0)$ to the conditions

$$\Gamma_{\text{cross}}^{11} = \mathcal{O}(N^{-2}), \quad \Gamma_{\text{cross}}^{12} = \mathcal{O}(N^{-1}), \quad (\text{C.3})$$

which are in accordance with (5.45). Let us consider the projection of the Wilson lines W_1 and W_2 onto the color structure $\delta_{i'j'}\delta_{j'i}$

$$(W_1)_{ij}^{i'j'}\delta_{i'j'}\delta_{j'i} = Nw'_1, \quad (W_2)_{ij}^{i'j'}\delta_{i'i}\delta_{j'j} = N^2w'_2, \quad (\text{C.4})$$

and repeat the large N analysis for the Wilson loops w'_1 and w'_2 . After substitution of (C.4) into the RG equation (2.10) we get

$$\mathcal{D}w'_2 = \frac{1}{N}\Gamma_{\text{cross}}^{21}w'_1 + \Gamma_{\text{cross}}^{22}w'_2, \quad (\text{C.5})$$

where \mathcal{D} denotes the RG operator. The Wilson loop w'_1 satisfies analogous relation. As in the previous case, the Wilson loops w'_2 is factorized in the large N limit into the product of two vacuum averaged Wilson loops evaluated along the paths having a cusp with the same angle γ introduced before. As a result, in the large N limit w'_2 has cusp singularities which are renormalized multiplicatively. This means, that, up to $\mathcal{O}(N^{-2})$ corrections, w'_2 should obey the homogeneous RG equation with the anomalous dimension $\frac{2C_F}{C_A}\Gamma_{\text{cusp}}(\gamma, g)$ equal to the cusp anomalous dimension defined in the *fundamental* representation of the $SU(N)$ times the number of cusps ($= 2$) with $C_F = (N^2 - 1)/(2N)$ and $C_A = N$. Since the Wilson loops w'_1 and w'_2 behave as $\mathcal{O}(N^0)$, this condition together with (C.5) implies that

$$\Gamma_{\text{cross}}^{21} = \mathcal{O}(N^{-1}), \quad \Gamma_{\text{cross}}^{22} = \Gamma_{\text{cusp}}(\gamma, g) + \mathcal{O}(N^{-2}) \quad (\text{C.6})$$

with $\Gamma_{\text{cusp}}(\gamma, g)$ defined in the adjoint representation of the $SU(N)$. Thus, in the large N limit the matrix $\Gamma_{\text{cross}}(\gamma, g)$ is given by (C.3) and (C.6) to all orders of PT.

References

- [1] P.D.B. Collins, “*An introduction to Regge theory and high energy physics*”, Cambridge Univ. Press (1977) 445.
- [2] E.A. Kuraev, L.N. Lipatov and V.S. Fadin, Sov.Phys.JETP 44 (1976) 443-451; 45 (1977) 199;
Ya.Ya. Balitskii and L.N. Lipatov, Sov.J.Nucl.Phys. 28 (1978) 822.
- [3] H. Cheng and T.T. Wu, “*Expanding Protons: Scattering at High Energies*”, (MIT Press, Cambridge, Massachusetts, 1987).
- [4] J. Bartels, Nucl. Phys. B175 (1980) 365.
- [5] L.N. Lipatov, Nucl. Phys. B365 (1991) 614.
- [6] L.N. Lipatov, Nucl. Phys. B309 (1988) 379; in “*Perturbative QCD*”, ed. A.H. Mueller (World Scientific, Singapore, 1989).
- [7] L.N. Lipatov, Padova preprint DFPD-93-TH-70; JETP Lett. 59 (1994) 596.
- [8] L.D. Faddeev and G.P. Korchemsky, Stony Brook preprint, ITP-SB-94-14, hep-th@xxx/9404173
- [9] H. Verlinde and E. Verlinde, Princeton Univ. preprint PUPT-1319, hep-th@xxx/9302104.
- [10] M.G. Sotiropoulos and G. Sterman, Nucl. Phys. B419 (1994) 59.
- [11] G.P. Korchemsky, Phys. Lett. B325 (1994) 459.
- [12] A.A. Migdal, Phys. Rep. 102 (1983) 199.
- [13] G.P. Korchemsky and A.V. Radyushkin, Sov. J. Nucl. Phys. 44 (1986) 145; 45 (1987) 127; 910; Phys. Lett. B171 (1986) 459; B279 (1992) 359;
G.P. Korchemsky, Phys. Lett. 217B (1989) 330; 220B (1989) 629; Mod. Phys. Lett. A4 (1989) 1257.
- [14] H. Cheng and T.T. Wu, Phys. Rev. Lett. 22 (1969) 666;
H. Abarbanel and C. Itzykson, Phys. Rev. Lett. 23 (1969) 53.
- [15] R.A. Brandt, F. Neri and M.-A. Sato, Phys. Rev. D24 (1981) 879;
R.A. Brandt, A. Gocksch, M.-A. Sato and F. Neri, Phys. Rev. D26 (1982) 3611.
- [16] A.M. Polyakov, Nucl. Phys. B164 (1980) 171.
- [17] I.Ya. Aref’eva, Phys. Lett. B93 (1980) 347;
V.S. Dotsenko and S.N. Vergeles, Nucl. Phys. B169 (1980) 527.
- [18] H.T. Nieh and Y.-P. Yao, Phys. Rev. Lett. 32 (1974) 1074; Phys. Rev. D13 (1976) 1082;
B.M. McCoy and T.T. Wu, Phys. Rev. Lett. 35 (1975) 604; Phys. Rev. D12 (1975) 3257;
L. Tyburski, Phys. Rev. D13 (1976) 1107;
C.Y. Lo and H. Cheng, Phys. Rev. D13 (1976) 1131.

[19] J.C. Collins and D. Soper, Nucl. Phys. B197 (1982) 446.

[20] G.P. Korchemsky and A.V. Radyushkin, Nucl. Phys. B283 (1987) 342.

Figures:

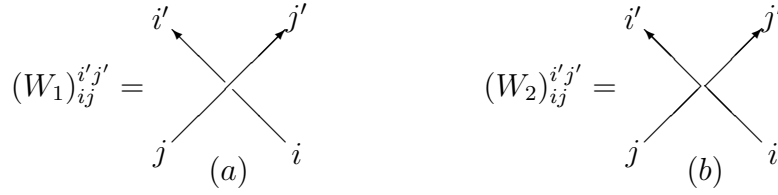


Fig.1: Integration paths (a) and (b) entering into the definition of the Wilson lines W_1 and W_2 , respectively.

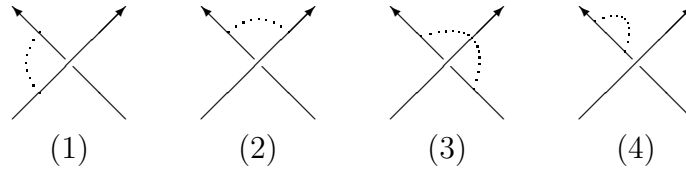


Fig.2: One-loop diagrams contributing to the line function W_1 . Solid line represents the integration path, dotted lines denote gluons.

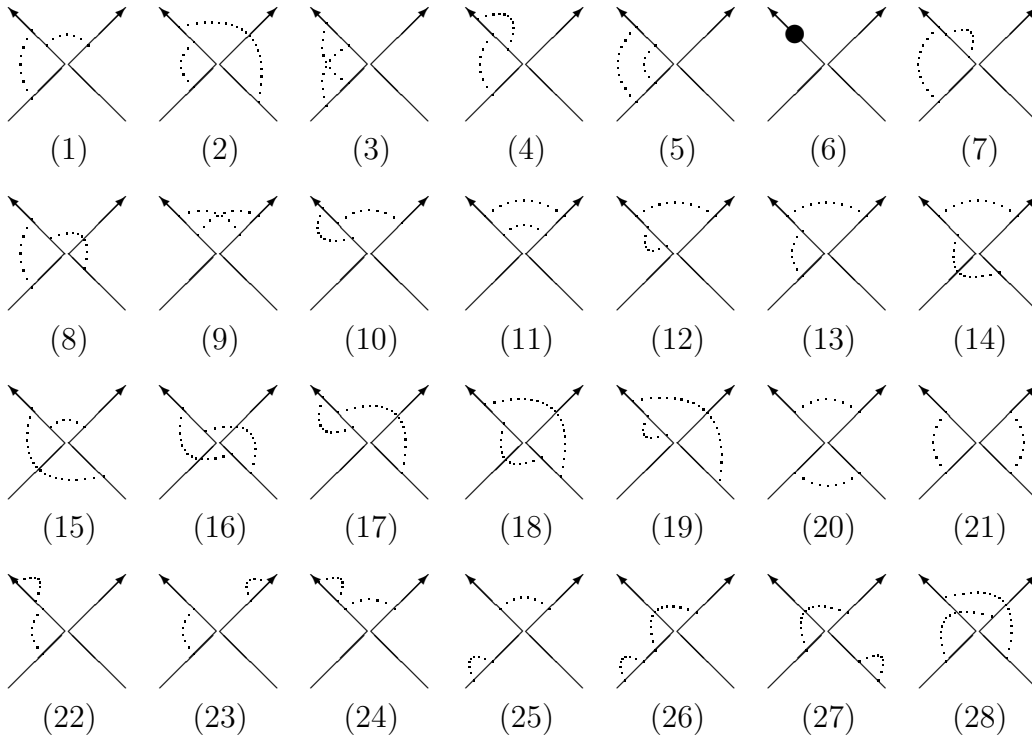


Fig.3: Two-loop QED like diagrams contributing to the line function W_2 . The blob in the diagram (6) denotes all possible QED like “self-energy” corrections to the Wilson line.

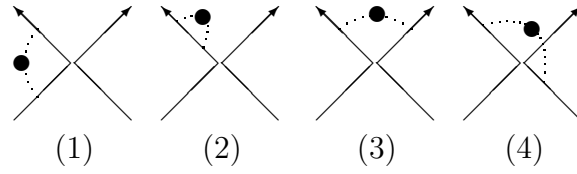


Fig.4: Two-loop self-energy diagrams. The blob denotes one-loop self-energy corrections to the gluon propagator.

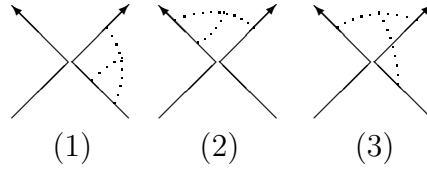


Fig.5: Two-loop three gluon diagrams.